

APPLICATION OF THE CELLULAR METHOD TO THE BAND
STRUCTURE OF ALUMINIUM

Thesis submitted to the University of London for the M.Sc. degree by
Daphne Joan Hall.

ProQuest Number: 10097237

All rights reserved

INFORMATION TO ALL USERS

The quality of this reproduction is dependent upon the quality of the copy submitted.

In the unlikely event that the author did not send a complete manuscript and there are missing pages, these will be noted. Also, if material had to be removed, a note will indicate the deletion.



ProQuest 10097237

Published by ProQuest LLC(2016). Copyright of the Dissertation is held by the Author.

All rights reserved.

This work is protected against unauthorized copying under Title 17, United States Code.
Microform Edition © ProQuest LLC.

ProQuest LLC
789 East Eisenhower Parkway
P.O. Box 1346
Ann Arbor, MI 48106-1346

A b s t r a c t.

A calculation of a few energy levels in the band structure of Aluminium by the cellular method.

A c k n o w l e d g m e n t .

I am greatly indebted to Dr. L. Pincherle for constant help and advice during the course of this investigation.

Contents.

| | | |
|-----------|--|-----------|
| | Introduction. | Page 1. |
| Chapter I | The Brillouin Zone of Aluminium. | 2. |
| II | The Band Structure in the Almost-Free Electron Approximation. | 7. |
| III | The Band Structure of Aluminium. | 13. |
| IV | The Cellular Method Calculation. | 18. |
| V | The Wave Functions & their Symmetry Properties. | 24. |
| VI | The Potential in the Atomic Cell. | 36. |
| VII | Numerical Calculation & Results. | 43. |
| | Conclusion | 52 |
| | Appendix | (i)-(xvi) |

I N T R O D U C T I O N.

The band structure of aluminium has recently been fully investigated by Heine (1957) using the orthogonalised plane wave method. A calculation based upon Heine's results shows that the actual band structure is very close to that obtained by an almost-free-electron approximation.

The object of the present calculation has been to recalculate the energies of a few points of interest in the Brillouin Zone by a simple application of the cellular method with Kohn's variational form of the surface matching conditions. The results therefore provide an estimate of the value of a cellular method calculation with the best possible matching conditions, when a limited number of terms are used in the expansion in spherical harmonics of the wave functions of almost-free electrons.

Chapter I. The Brillouin Zone of Aluminium.

For electrons in a periodic potential the wave functions are, by Bloch's theorem

$$\psi(\underline{k}, \underline{r}) = \exp(i\underline{k} \cdot \underline{r}) u(\underline{k}, \underline{r}) \quad (1)$$

where $u(\underline{k}, \underline{r})$ is a function having the periodicity of the lattice, and \underline{k} is a real vector with dimensions \underline{p}/\hbar , \underline{p} being the momentum of the electron. From this equation it follows that the wave function at any point of the crystal may be deduced from a knowledge of the wave functions of a single cell of the lattice. This is the basis of the cellular method.

The vector \underline{k} is not fully defined by equation (1).

Without changing the meaning of the equation one may add to \underline{k} a vector \underline{K} such that

$$\underline{K} \cdot \underline{a}_1 = 2\pi n_1; \quad \underline{K} \cdot \underline{a}_2 = 2\pi n_2; \quad \underline{K} \cdot \underline{a}_3 = 2\pi n_3 \quad (2)$$

where $\underline{a}_1, \underline{a}_2, \underline{a}_3$ are the three primitive displacements of the direct lattice, and n_1, n_2, n_3 are integers. This will merely introduce a factor periodic in \underline{r} into the R.H.S. of equation (1), and this may be absorbed into $u(\underline{r}, \underline{k})$.

The vectors \underline{K} satisfying equations (2) may be regarded as fundamental translation vectors $2\pi(n_1, n_2, n_3)$ lying in a reciprocal lattice which has primitive displacement vectors defined by

$$\underline{a}_i \cdot \underline{b}_j = 2\pi \delta_{ij}$$

or explicitly,

$$\underline{b}_1 = \frac{2\pi}{\underline{a}_1 \cdot \underline{a}_2 \wedge \underline{a}_3} \underline{a}_2 \wedge \underline{a}_3; \quad \underline{b}_2 = \frac{2\pi}{\underline{a}_1 \cdot \underline{a}_2 \wedge \underline{a}_3} \underline{a}_3 \wedge \underline{a}_1; \quad \underline{b}_3 = \frac{2\pi}{\underline{a}_1 \cdot \underline{a}_2 \wedge \underline{a}_3} \underline{a}_1 \wedge \underline{a}_2$$

Since equation (1) is not changed by changing \underline{k} to $(\underline{k} + \underline{K}_n)$, all points which are separated from \underline{k} by some multiple of a fundamental translation of the reciprocal lattice may be considered as equivalent to \underline{k} . A unit cell in \underline{k} -space may then be defined as that region which encloses all different vectors \underline{k} . This is the fundamental Brillouin Zone. In the Brillouin Zone the wave function will be a multivalued function of \underline{k} (by virtue of the change in $u(\underline{k}, r)$, the periodic part of $\psi(\underline{k}, r)$, which results from considering \underline{k} and $\underline{k} + \underline{K}_n$ identical). The energy $E(\underline{k})$ associated with the wave function will also be a multivalued function of \underline{k} .

The crystal of aluminium has a face-centred cubic structure with lattice parameter, $a = 4.041 \text{ \AA}$ ($= 7.648$ atomic units, where $1 \text{ a.u.} = \hbar^2 / me^2 = 0.5284 \times 10^{-8} \text{ cm}$).

Any Bravais lattice such as this may be specified by a matrix, A , with elements equal to the Cartesian components of the primitive lattice displacement vectors $\underline{a}_1, \underline{a}_2, \underline{a}_3$. (Fig. 1 (i))

$$A = \begin{pmatrix} 0 & \frac{a}{2} & \frac{a}{2} \\ \frac{a}{2} & 0 & \frac{a}{2} \\ \frac{a}{2} & \frac{a}{2} & 0 \end{pmatrix}$$

Any lattice displacement $\underline{n} = (n_1 \underline{a}_1 + n_2 \underline{a}_2 + n_3 \underline{a}_3)$ may then be written as the scalar product

$$A \cdot \underline{n} = \begin{pmatrix} 0 & \frac{a}{2} & \frac{a}{2} \\ \frac{a}{2} & 0 & \frac{a}{2} \\ \frac{a}{2} & \frac{a}{2} & 0 \end{pmatrix} \begin{pmatrix} n_1 \\ n_2 \\ n_3 \end{pmatrix} = n_1 \underline{a}_1 + n_2 \underline{a}_2 + n_3 \underline{a}_3$$

and the separation of the two points $\underline{n}, \underline{m}$ simply as

$$A \cdot (\underline{n} - \underline{m}) = 0 \quad \begin{pmatrix} \frac{a}{2} & \frac{a}{2} & 0 \\ \frac{a}{2} & 0 & \frac{a}{2} \\ \frac{a}{2} & \frac{a}{2} & 0 \end{pmatrix} \begin{pmatrix} n_1 - m_1 \\ n_2 - m_2 \\ n_3 - m_3 \end{pmatrix}$$

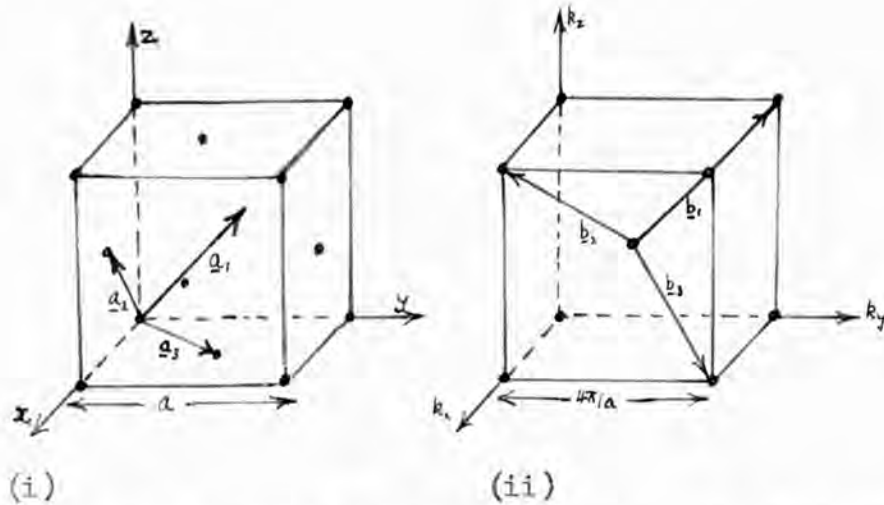


Fig. I. Unit Cells of Direct and Reciprocal Lattices.

The reciprocal lattice defined by equations (2) is body-centred cubic with a matrix representation, B (Fig. I (ii)).

$$B = 2\pi \begin{pmatrix} \frac{1}{a} & \frac{1}{a} & \frac{1}{a} \\ \frac{1}{a} & -\frac{1}{a} & \frac{1}{a} \\ \frac{1}{a} & \frac{1}{a} & -\frac{1}{a} \end{pmatrix}$$

For such structures, the smallest cell, which under all possible lattice translations will build up the whole crystal is the smallest volume enclosed by planes which bisect perpendicularly the shortest translation vectors joining any given lattice point to its neighbours. In the direct lattice (f.c.c.) these are the planes

$$\underline{r} \cdot (\underline{A} \cdot \underline{n}) = \frac{1}{2} |\underline{A} \cdot \underline{n}|^2$$

bisecting the twelve vectors, $\underline{n} = (0 \pm \frac{1}{2} \pm \frac{1}{2})$ $\underline{n} = (\pm \frac{1}{2} 0 \pm \frac{1}{2})$

$\underline{n} = (\pm \frac{1}{2} 0 \pm \frac{1}{2} 0)$, of equal length joining a lattice point to its twelve nearest neighbours. The atomic cell formed by these planes is the rhombododecahedron of Fig.2 (i)

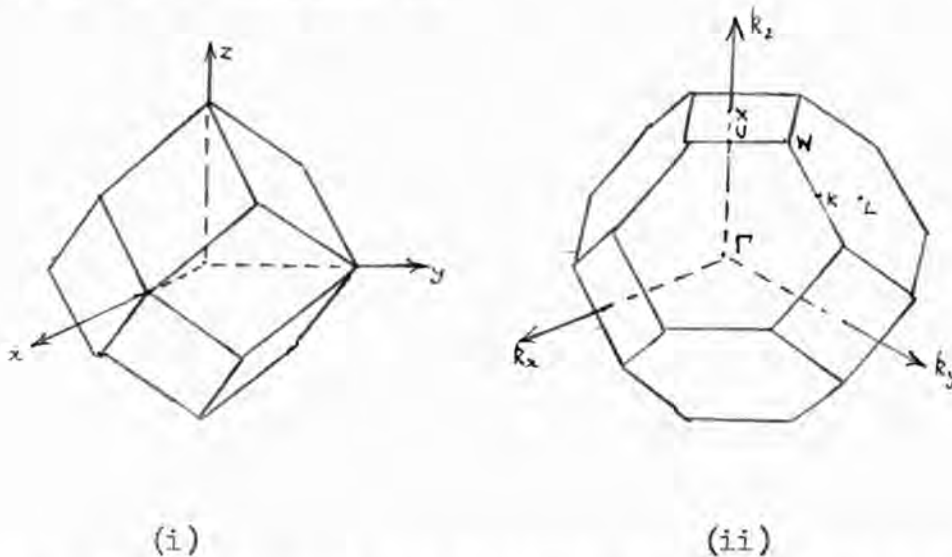


Fig. 2. The Atomic Cell and Brillouin Zone for Aluminium.

In the body centred cubic lattice the cell is the truncated octahedron of Fig. 2 (ii) defined by the planes

$$\underline{k} \cdot (\underline{B} \cdot \underline{n}') = \frac{1}{2} |\underline{B} \cdot \underline{n}'|^2$$

bisecting the eight nearest neighbours vectors $\underline{n}' = (\pm 1 \pm 1 \pm 1)$ passing through the hexagonal faces, and the six next-nearest neighbour vectors $\underline{n}' = (\pm 2 0 0)$ $\underline{n}' = (0 \pm 2 0)$ $\underline{n}' = (0 0 \pm 2)$ passing through the square faces. This is the atomic cell for a b.c.c. lattice, and the Brillouin Zone for the f.c.c. lattice (though it may be shown that it is not an unique choice in this case), with opposite faces separated by distances equal to the lengths of the vectors of the

two types of fundamental reciprocal lattice displacements.

$$\text{Distance between nearest neighbours} = \frac{2\pi\sqrt{3}}{a}$$

$$\text{Distance between next nearest neighbours} = \frac{4\pi}{a}$$

Points of high symmetry in the zone are labelled. These are the centre, Γ , ($\underline{k} = \frac{\pi}{a} (0, 0, 0)$), the centre of the square face, X,

($\underline{k} = \frac{\pi}{a} (0, 0, 2)$), the mid-point of the hexagonal face L ($\underline{k} = \frac{\pi}{a} (1, 1, 1)$),

the corner point W ($\underline{k} = \frac{\pi}{a} (0, 1, 2)$) and the mid points of the sides,

K or U ($\underline{k} = \frac{\pi}{a} (0, \frac{3}{2}, \frac{3}{2})$) and $\underline{k} = \frac{\pi}{a} (\frac{1}{2}, \frac{1}{2}, 2)$).

Chapter II. The Band Structure in the Almost-Free Electron Approximation.

In an arbitrary, constant potential, V_0 , the wave functions of free electrons are the plane waves

$$\psi_{n\mathbf{k}}(\underline{r}) = \frac{1}{\sqrt{N\Omega}} e^{i(\underline{k} + \underline{K}_n) \cdot \underline{r}} \quad (1)$$

where N is the number of atomic cells each of volume Ω in the metal, and \underline{K}_n is the reciprocal lattice displacement vector associated with the n th branch of the $E(\underline{k}) - (\underline{k})$ distribution.

The free electron energies are

$$E_{n\mathbf{k}} = \hbar^2/2m (\underline{k} + \underline{K}_n)^2 + V_0. \quad (2)$$

Consider the addition to V_0 of a small periodic perturbing potential $V(\underline{r})$.

$$V(\underline{r}) = \sum_{n=-\infty}^{\infty} V_n e^{i\mathbf{K}_n \cdot \underline{r}}.$$

with Fourier components

$$V_n = \frac{1}{\Omega} \int V(\underline{r}) e^{-i\mathbf{K}_n \cdot \underline{r}} d\underline{r}.$$

The perturbed energies, E , will be the roots of secular equation

$$\text{Det} | H_{mn} - E \delta_{mn} | = 0 \quad (3)$$

where H_{mn} are the matrix elements of the Hamiltonian

$$H = -\hbar^2/2m \nabla^2 + V_0 + V(\underline{r})$$

It may be shown that a ^{non-vanishing} matrix element $(\underline{k}_m | V | \underline{k}_n)$ of $V(\underline{r})$ only exists

between the unperturbed functions $\frac{1}{\sqrt{N\Omega}} e^{i\mathbf{k}_n \cdot \underline{r}}$ and $\frac{1}{\sqrt{N\Omega}} e^{i\mathbf{k}_m \cdot \underline{r}}$ when

their wave vectors differ by a displacement vector of the reciprocal lattice

$$\underline{k}_n - \underline{k}_m = B \cdot \underline{l}$$

In this case, the matrix element V_{mn} is simply the Fourier coefficient of the potential

$$(\underline{k}_m | V | \underline{k}_n) = V_{m-n} = V_l.$$

All the elements V_l belonging to the set $l = \{l_1, l_2, l_3\}$ are equal. Consider a point, for example the point X, on the zone boundary (Fig. 2(ii)). On the nth branch this is the point

$$(\underline{k} + \underline{K}_n) = \frac{2\pi}{a} (1, 0, 0) + \underline{K}_n$$

The wave functions of the point

$$(\underline{k}' + \underline{K}_{n+1}) = \frac{2\pi}{a} (-1, 0, 0) + \underline{K}_{n+1}$$

which is degenerate with $(\underline{k} + \underline{K}_n)$ in the unperturbed state, will combine with those at $(\underline{k} + \underline{K}_n)$, since

$$(\underline{k} + \underline{K}_n) - (\underline{k}' + \underline{K}_{n+1}) = B \cdot \underline{l} = \frac{2\pi}{a} (2, 0, 0)$$

giving a non-vanishing matrix element V_{200} .

To a first order approximation, since $V(\underline{r})$ is itself small, other Fourier coefficients arising from combinations with $(\underline{k} + \underline{K}_n)$ of states on other branches, n' , ($n' \neq n$) of the $E(\underline{k}) - (\underline{k})$ curve will be negligible.

Equation (3) becomes

$$\begin{vmatrix} + \frac{\hbar^2}{2m} (\underline{k} + \frac{K}{n}) + V_0 - E & V_{200} \\ V_{200} & + \frac{\hbar^2}{2m} (\underline{k} + \frac{K}{n}) + V_0 - E \end{vmatrix} = 0$$

with 2 roots

$$E = \frac{\hbar^2}{2m} (\underline{k} + \frac{K}{n})^2 + V_0 \pm |V_{200}|$$

The periodic potential has therefore separated the two levels, originally degenerate at X, by an amount

$$\Delta E = 2|V_{200}|$$

The continuous $E(\underline{k}) - (\underline{k})$ distribution throughout the n branches of the Brillouin zone, of the free electron case, becomes modified into a band scheme, with regions ΔE of forbidden energies separating the bands at the zone boundary.

At the point K there are three degenerate levels in the unperturbed state

$$\underline{k}_1 = \frac{2\pi}{a} (1, \frac{1}{4}, \frac{1}{4}); \quad \underline{k}_2 = \frac{2\pi}{a} (-1, \frac{1}{4}, \frac{1}{4}); \quad \underline{k}_3 = \frac{2\pi}{a} (0, -\frac{3}{4}, -\frac{3}{4})$$

giving, in the first order approximation, three non-vanishing matrix elements of V

$$V_{12} = V_{200}; \quad V_{13} = V_{111}; \quad V_{23} = V_{111} = V_{111}$$

The resulting secular equation has three distinct roots, the degeneracy of the 3 unperturbed bands at K being completely lifted by the periodic potential $V(\underline{r})$.

The energies of the points X, K(= U) and W in the almost-free electron approximation are listed in table (1). (taking $V_0 = 0$ and $\frac{K}{n} = 0$).

Since the exact energies at these points are available from Heine's results, (table 2, col. (i)), the Fourier coefficients V_{200} and V_{111} may be calculated from the energy gaps, ΔE . From table (1) the energy of any point may then be recalculated in the almost-free electron approximation. The results of such a calculation are shown in table (2) col. (ii) together with exact results of Heine (col. (i)).

| Point | Energy | Band |
|-------|---|------|
| X | $\frac{\hbar^2 k^2}{2m} - V_{200}$ | 1 |
| | $\frac{\hbar^2 k^2}{2m} + V_{200}$ | 2 |
| K(=U) | $\frac{\hbar^2 k^2}{2m} - V_{200}$ | 1 |
| | $\frac{\hbar^2 k^2}{2m} + \frac{V_{200} - (V_{200}^2 + 8V_{111}^2)^{1/2}}{2}$ | 2 |
| | $\frac{\hbar^2 k^2}{2m} - \frac{V_{200} - (V_{200}^2 + 8V_{111}^2)^{1/2}}{2}$ | 3 |
| W | $\frac{\hbar^2 k^2}{2m} - V_{200}$ | 1,2 |
| | $\frac{\hbar^2 k^2}{2m} - 2V_{111}$ | 3 |
| | $\frac{\hbar^2 k^2}{2m} + 2V_{111}$ | 4 |

Table 1. Energies at points of high symmetry on the zone boundary, (almost-free electron approximation).

Then

$$\text{At X} \quad E = 2V_{200} = .123 \text{ Ry.}$$

$$\text{At W} \quad E = 4V_{111} = .119 \text{ Ry.}$$

$$V_{200} = .061 \text{ Ry.}$$

$$V_{111} = .030 \text{ Ry.}$$

Substitution of these values into table 1 gives the results listed in Table 2, col.(ii). The free electron correlation energy, V_{EP} , included in Heine's results (cf. ch.VI) has also been included in the results of column (ii) for the purposes of comparison.

| Point | Energy (Heine) | Almost-free electrons | Band |
|-------|----------------|-----------------------|-------|
| X | .806 Ry. | .825 Ry. | 1 |
| | .929 | .950 | 2 |
| K | .925 | .936 | 1 |
| | .966 | .946 | 2 |
| | 1.298 | .988 | 3 |
| W | 1.012 | 1.018 | 1,2 |
| | 1.063 | 1.019 | 3 |
| | 1.182 | 1.137 | 4 |
| | (i) | (ii) | (iii) |

Table 2. Energies at points of the Brillouin Zone.

The energies are within 0.05 Ry. of Heine's results, except for a surprising discrepancy (0.3 Ry.) at K in the third band, so that

the almost-free electron approximation gives a fairly satisfactory account of the band structure of aluminium.

Chapter III. The Band Structure of Aluminium.

It is of interest here to summarise the model of the band structure of aluminium which Heine has built up from the available experimental data, from the theoretical results for points of high symmetry given in the previous chapter and from the energies at 140 more-general points in the zone which are estimated to be not more than 0.01 Ry. from their final self-consistent value.

Throughout almost the whole of k -space, the energy surfaces are within about 0.01 Ry. of the spheres associated with free electrons of effective mass 1.03. This is true for k up to within 0.05 a.u. from a zone-face (for comparison $L = 0.71$ a.u. + $X = 0.82$ a.u.). In the neighbourhood of the zone surfaces it has been shown that the behaviour is fairly well represented by an almost-free electron model.

For free electrons with effective mass 1.03 in a metal with 3 valence electrons per atom the Fermi energy is 1.084 Ry. which is greater than all the energies calculated for the first zone. The simplest interpretation of the band structure is therefore that of spherical energy surfaces filling all states up to a Fermi energy of 1.084 Ry. which occurs somewhere in the second band. However, such a model disagrees rather badly with the experimental information which for aluminium relates chiefly to measurements of the electronic specific heat, the anomalous skin effect, and the de Haas - van Alphen effect.

The Electronic Specific Heat.

Specific heat measurements give a mean value for the density of states $n(E)$ in energy at the Fermi surface of 0.071 states/unit volume_{per a.u. of energy} of the metal, in comparison with 0.041 states/unit volume/a.u.

for the free electron distribution. Since

$$n(E) = \frac{1}{4\pi^3} \int \frac{dS}{\text{grad}_{\underline{k}} E} \quad (1)$$

(c.f. Mott and Jones p.88) where the integration extends over the whole Fermi surface, there must be some regions of the Fermi surface where the value of $n(E)$ is very high on account of a low value of $\text{grad}_{\underline{k}} E$. Such regions will occur if the Fermi surface approaches closely one of the zone faces. It seems likely therefore that some part of the Fermi surface will cut the zone boundaries and further calculations suggest that this occurs near the corners, W.

The Anomalous Skin Effect.

It may be shown (Pippard 1954) that, for a very pure polycrystalline material in the extreme anomalous limit when the skin depth is small in comparison with the mean free path of the electrons, the average value of the surface resistance measured over all perpendicular directions, x and y , is given by

$$\frac{1}{R_x} + \frac{1}{R_y} = \frac{4e^2 S}{27\pi \omega \hbar^3} \quad (2)$$

where S is the total area of the Fermi surface, $\hbar = (1/8\pi)^{1/3}$ and ω is the field angular frequency. Measurements therefore lead to an estimate of the total area of the Fermi surface. For aluminium the available measurements, which may be 20% in error, give almost the same value for S as that of a free electron distribution with 3 electrons per atom. Thus, if crossing of the zone boundaries does occur, it will probably occur only to a very small extent, with practically the whole of the Fermi surface corresponding to a free electron distribution.

The de Haas - van Alphen Effect.

In the case of aluminium, the de Haas - van Alphen effect yields the most valuable of the experimental information on the band structure.

At liquid helium temperatures, the magnetic susceptibility X becomes quasi-periodic with the magnetic field $\frac{1}{H}$ with period of oscillation P

$$P = \frac{4\pi^2 e}{chA} \quad (3)$$

measured in Gaussian units of $\frac{1}{H}$ (Gunnarsen 1957). Here, A is the area in k -space of the maximum cross section, measured perpendicular to the magnetic field, of a closed region of the Fermi surface.

The number of electrons in such a closed region will be determined by its volume. Their effective mass may, in principle, be deduced from the magnitude of the field which is necessary in order to give oscillations of measurable amplitude.

In aluminium, two separate oscillations are observed. Another very high frequency oscillation which, on this model for the band structure, may be expected to arise from the main region of the Fermi sphere in the second band, have not yet been observed experimentally, with the field strengths available.

Of the observed oscillations (Gunnarsen 1957), there is a set with high frequency of which Heine has made an exhaustive study. From symmetry considerations he shows that they probably belong to pockets of holes or electrons placed at the 24 corners, W , of the zone. These join up under ~~the~~ four fundamental translations associated with ~~the four~~ ^(f, 3, 2, 4) points W (cf. Ch.V) to give three pairs of closed surfaces, each containing 0.6×10^{-3} electrons or holes per atom, and each with cross-section A given by equation (3). Since the pockets of each pair are

inversion images of each other, they give rise to oscillations of equal period for all directions of the magnetic field H , and the shape which is deduced from measurements of A over all directions of H is that of a symmetrical combination of the two pockets. For a single pocket, the actual shape, which is determined by the energy surfaces in the neighbourhood of W , is cushion-like with an approximate mean radius of 0.06 a.u.

Pockets of holes occurring in the first band seem to be more consistent with the observed shape than pockets of electrons in the third band. Heine has reached this conclusion by detailed consideration of the possible band structures in the neighbourhood of which W would result from various arbitrary arrangements of the first four bands at W relative to each other and to the Fermi surface. In no case is the agreement with experiment conclusive. The results obtained from the orthogonalised plane waves calculation (Table 1 p.11) lead to fairly consistent results, but the interpretation of the experimental data cannot be said to have been finally decided.

It appears therefore that there are unoccupied states in the first zone at W even though it lies below the Fermi surface. To explain this, Aigrain has suggested that "it is possible that correlation between these holes in the electron distribution, and the electron gas itself may sometimes lead to a lowering of the total energy to a value below that occurring for a filled band."

A low frequency oscillation is also observed. Alloying with magnesium which has two valence electrons per atom reduces the electron density, and also the frequency of the oscillations. The oscillations therefore arise from pockets of electrons, each

containing 3.6×10^{-5} electrons per atom, which are probably in the third band. Heine has not investigated these fully but suggests that they may be located near W, where a line of contact between the second and third bands occurs along which the energy may fall just below the Fermi level. The almost free electron calculation of Chapter 2 suggests, on the other hand, that these pockets will occur near the points K in the Brillouin Zone. This has also been noted by Herman (1958). The final model for the band structure which has therefore been adopted is; in the first and second bands, spherical energy surfaces with effective mass 1.03 up to a Fermi level of 1.084 Ry. except near W where a few states are left unoccupied in both bands (degenerate at W); in the third band, a very small concentration of electrons where the energy falls below the Fermi level. The fourth zone is probably completely empty.

In view of the uncertainty in the situation at W, this point was selected for the present calculations. It was thought that this would provide a further theoretical confirmation of the interpretation of the experimental results.

Chapter IV. The Cellular Method Calculation.

It was pointed out above (Ch.I) that by virtue of Bloch's theorem, the problem of finding the electronic wave functions and energies may be solved completely by considering only a single cell of the crystal lattice. To do this, Schrodinger's equation

$$(-\nabla^2 + V(\underline{r}) - \lambda(k))\psi(\underline{r}) = 0 \quad (1)$$

must be solved subject to the Bloch periodic condition

$$\psi(\underline{r}') = \exp(i\mathbf{k} \cdot \underline{\tau}_r) \psi(\underline{r}) \quad (2)$$

and subject also to the condition that the wave function must, by the continuity of the normal derivative $\nabla_n \psi(\underline{r})$ across the cell boundary, join on smoothly to the solutions in neighbouring cells.

$$\nabla_n \psi(\underline{r}') = - \exp(i\mathbf{k} \cdot \underline{\tau}_r) \nabla_n \psi(\underline{r}) \quad (3)$$

In these equations $V(\underline{r})$ is the crystal potential and λ is the energy of the state \mathbf{k} . The vector $\underline{\tau}_r = (\underline{r}' - \underline{r})$ is the fundamental lattice displacement vector between conjugate points \underline{r} and \underline{r}' on opposite faces of the atomic cell. The negative sign appears in equation (3) if by ∇_n is understood differentiation along the outward normal at any point (\underline{r}) .

If the potential distribution $V(\underline{r})$ is assumed to be spherically symmetrical about the atom at the centre of the cell, then Schrodinger's equation becomes separable with solutions

$$\psi(\underline{r}) = \sum_{l, m} A_{l, m} \varphi_l(r, \lambda) \quad (4)$$

$$\varphi_l(r, \lambda) = Y_l^m(\cos \theta) R_l(r, \lambda) \quad (5)$$

where $Y_l^m(\cos \theta)$ is a surface harmonic, and $R_l(r; \lambda)$ the radial function, governed by the equation

$$\frac{dP}{dr} + (\lambda - V(r) - \frac{l(l+1)}{r^2})P = 0 \quad P = rR \quad (6)$$

associated with a particular energy, λ , and a particular choice of the azimuthal quantum number, l . The coefficients A_{lm} will be determined by satisfying equations (2) and (3) at all points of the cell boundary. In practice this cannot be done exactly because the labour involved in taking into account more coefficients A_{lm} than are contained in the expansion of ψ carried up to only a fairly low value of l becomes too great.

Various approximate methods have been developed for determining the coefficients A_{lm} and the energy eigenvalues $\lambda(\underline{k})$. In principle, these consist in satisfying the boundary conditions at a limited number of points over the surface and applying weight factors to the energies obtained from various combinations of such points to give an average value $\lambda(\underline{k})$, for the state.

In this calculation, the variational procedure for periodic lattices of Kohn has been adopted. In this method, all points on all faces of the cell are matched simultaneously, the weighting factors being derived from a surface integration formula (v.Ch.VII). Provided the integration is carried out over a sufficiently fine network of points, the method should lead to the best possible value of the energy which can be obtained from a wave function containing only a limited number of terms.

The variational procedure has been developed for composite lattices by several authors. In this calculation, it is applied to the relatively simple case of a Bravais lattice with all the atomic polyhedra translationally equivalent.

The Variational Principle.

In order to use the variational method we must set up a variation functional which will impose all the required conditions upon the wave function. These are the conditions of equations (1), (2) and (3), above

$$(-\nabla^2 + V(\underline{r}) - \lambda)\psi(\underline{r}) = 0 \quad (1)$$

for all \underline{r} inside the polyhedron

$$\psi(\underline{r}') = \exp(i\underline{k} \cdot \underline{r}_T) \psi(\underline{r}) \quad (2)$$

and

$$\nabla_n \psi(\underline{r}') = - \exp(i\underline{k} \cdot \underline{r}_T) \nabla_n \psi(\underline{r}) \quad (3)$$

for all \underline{r} on the surface of the polyhedron.

Consider first the functional

$$I = \int_{\Omega} \psi^* (-\nabla^2 + V(\underline{r}) - \lambda(\underline{k})) \psi d\omega \quad (7)$$

where Ω = the volume of the atomic cell.

$$\delta I = \delta \int_{\Omega} \psi^* (-\nabla^2 + V(\underline{r}) - \lambda(\underline{k})) \psi d\omega \quad (8)$$

Since the integration is not over the whole of space, in general δI will not vanish.

To find an expression for δI in terms of the boundary conditions (2) and (3), equation (7) may be transformed using Green's theorem and equation (1) for both ψ and ψ^* .

$$\begin{aligned} \delta I &= \int_{\Omega} \delta \psi^* (-\nabla^2 + V(\underline{r}) - \lambda(\underline{k})) \psi d\omega + \int_{\Omega} \psi^* (-\nabla^2 + V(\underline{r}) - \lambda(\underline{k})) \delta \psi d\omega \\ &= \int_{\Omega} (-\psi^* \nabla^2 \delta \psi + \psi^* (V(\underline{r}) - \lambda(\underline{k})) \delta \psi) d\omega \end{aligned}$$

$$\begin{aligned}
 &= \int_{\Omega} (-\psi^* \nabla^2 \delta\psi + \nabla^2 \psi^* \delta\psi) d\omega \\
 &= \int_S (\delta\psi \nabla_n \psi^* - \psi^* \nabla_n \delta\psi) dS
 \end{aligned} \tag{9}$$

where S = the surface area of the atomic cell.

Taking the real part of the 1st term of equation (9)

$$\begin{aligned}
 \operatorname{Re} \int_S \delta\psi(\underline{r}) \nabla_n \psi^*(\underline{r}) dS &= \operatorname{Re} \int_S \nabla_n \psi(\underline{r}) \delta\psi^*(\underline{r}) dS \\
 &= \operatorname{Re} \int_S \nabla_n \psi(\underline{r}') \delta\psi^*(\underline{r}') dS \\
 &= \operatorname{Re} \int_S -\nabla_n \psi(\underline{r}) \delta\psi^*(\underline{r}') \exp(i\mathbf{k} \cdot \underline{\tau}_r) dS
 \end{aligned}$$

from equation (2)

By a similar transformation using equation (3), the second term of equation (9) (real part) may be written

$$\operatorname{Re} \int_S -\psi^*(\underline{r}) \nabla_n \delta\psi(\underline{r}) dS = \operatorname{Re} \int_S -\nabla_n \delta\psi(\underline{r}) \psi^*(\underline{r}') \exp(i\mathbf{k} \cdot \underline{\tau}_r) dS$$

Hence the real part of equation (8) may be written

$$\delta(\operatorname{Re} I) = -\delta \operatorname{Re} \int_S \nabla_n \psi(\underline{r}) \psi^*(\underline{r}') \exp(i\mathbf{k} \cdot \underline{\tau}_r) dS \tag{10}$$

Subtracting equation (10) from the real part of equation (8)

$$\begin{aligned}
 0 &= \delta \operatorname{Re} \left[\int_{\Omega} \psi^*(\underline{r}) [-\nabla^2 + V(\underline{r}) - \lambda(\mathbf{k})] \psi(\underline{r}) d\omega + \int_S \nabla_n \psi(\underline{r}) \psi^*(\underline{r}') \exp(i\mathbf{k} \cdot \underline{\tau}_r) dS \right] \\
 &= \delta J(\psi, \mathbf{k}, \lambda)
 \end{aligned} \tag{11}$$

where δJ is the R.H.S. of equation (11).

We have thus found a functional J which has a stationary property for variations in ψ and vanishes for the correct $\psi(\underline{k}, \lambda)$. For arbitrary variations in ψ , not obeying all three equations (1), (2) and (3) separately, equation (11) will not, however, lead to an upper bound of λ .

In the spherical potential which we assume, the trial functions, ϕ , are always of a form which satisfies Schrodinger's equation and the first integral vanishes. The resulting variational equation is

$$J(\psi, \underline{k}, \lambda) = \text{Re} \int_S \psi^*(\underline{r}') \nabla_n \psi(\underline{r}) \exp(i\underline{k} \cdot \underline{r}_T) dS = \text{stationary.} \quad (12)$$

This will be solved for trial functions of the form

$$\psi(\underline{r}) = \sum_{l_m} A_{l_m} \phi_{l_m}(\underline{r}, \lambda') \quad (4)$$

by varying w.r.t. the coefficients A_{l_m} and solving the determinantal equation of the resulting set of linear equations for different choices of the trial energy, λ' .

For the points $\Gamma(k=0)$ and $W(k = \frac{\pi}{a}(1,2,0))$ (fig 2(ii))

for which calculations were made, the exponential term $\exp(i\underline{k} \cdot \underline{r}_T)$ is either purely real or purely imaginary on any face of the dodecahedron. Writing the wave function in terms of its odd and even expansions

$$\psi(\underline{r}) = u(\underline{r}) + iv(\underline{r})$$

equation (12) becomes

$$\begin{aligned}
 J(\psi, \underline{k}, \lambda) &= \sum_{\text{real } S} \int (u(\underline{r}') \nabla_n u(\underline{r}) - v(\underline{r}') \nabla_n v(\underline{r})) dS \\
 &+ \sum_{\text{imag. } S} \int (v(\underline{r}') \nabla_n u(\underline{r}) - u(\underline{r}') \nabla_n v(\underline{r})) dS \\
 &= \text{stationary}
 \end{aligned}
 \tag{13}$$

where the \sum_{real} denotes summation over all faces for which the exponential term is real and $\sum_{\text{imag.}}$ summation over those for which it is imaginary.

Equation (13) is the form of the variational principle which was used.

Chapter V. The Wave Functions and their Symmetry Properties.

In the cellular method, the translational symmetry of the crystal leads to the Bloch condition, which enables the problem to be completely solved in a single cell of the lattice. In this cell, the wave function is expanded in spherical harmonics, and one of the main approximations of the method lies in the necessity of neglecting all the harmonics of order greater than a rather low value of the azimuthal quantum number, l . This is because it becomes impracticable to deal with too large a number of unknown coefficients A_{lm} . For any given value of l , the number $(\sum_0^l (2l+1))$ of these coefficients may be substantially reduced by taking advantage of the rotational symmetry properties which also belong to the crystal.

Classification of the Wave Functions at a point in the Brillouin Zone.

Consider a wave function ϕ , associated with a point of the zone of wave vector \underline{k} and energy $E(\underline{k})$. Under the group $G(R)$ of the g operations (rotations and reflections) which bring the unit cell back into coincidence with itself, ϕ_1 will transform into $\phi_1, \phi_2 \dots \phi_s$ ($s \leq g$) with wave vectors $\underline{k}_1, \underline{k}_2 \dots \underline{k}_s$ respectively. These functions will all be eigenfunctions of the lattice Hamiltonian $H = -\nabla^2 + V(r)$ which is invariant under $G(R)$.

The wave functions associated with any of the rotationally equivalent points $\underline{k}_1, \underline{k}_2 \dots \underline{k}_s$ of the zone will be linear combinations $\psi_1, \psi_2 \dots \psi_s$ of these $\phi_1, \phi_2 \dots \phi_s$. Under any rotation, r , of $G(r)$ ψ_n will transform

$$r\psi_n = \sum_m r_{nm} \psi_m$$

where the coefficients r_{nm} form the elements of an s -dimensional matrix representation of the rotation with the wave functions $\psi_1,$

$\psi_2 \dots \psi_s$ as basis. Other rotations of the group will possess similar representations referred to the same basis.

In a band structure calculation, we are considering the wave functions associated with a fixed point \underline{k} in the Brillouin zone, and in this case, the number of the initial wave functions, ϕ_i will be restricted to those which transform into each other with the same or an equivalent value of \underline{k} . The rotations, r , for which this occurs form a subgroup, $G(\underline{k})$, of $G(R)$ - the group of \underline{k} . For a general \underline{k} , $G(\underline{k})$ will contain only one element, the identity; while for points of high symmetry in the zone it will contain a fairly large number.

In considering the symmetry restrictions on the wave functions it is therefore only necessary to consider the rotations in $G(\underline{k})$. It may be shown that a function transforming correctly under the subgroup $G(\underline{k})$ will always do so under the full rotation group $G(R)$.

Since the elements of $G(\underline{k})$ do not commute, all the representations $[r_{mn}]$ cannot be diagonalised simultaneously. However, they may be reduced by a suitable unitary transformation, or, equivalently, by a particular choice of the linear combinations $\psi_1, \psi_2 \dots \psi_s$, into direct sums of matrices of smaller dimensions. For example with the correct basis functions $[r_{mn}]$ may become expressible as

$$[r_{nm}] = \begin{pmatrix} [a_{11}] & 0 & 0 & - & - \\ 0 & \begin{bmatrix} b_{11} & b_{12} \\ b_{21} & b_{22} \end{bmatrix} & - & - & - \\ 0 & - & - & [c_{11}] & - \\ - & - & - & - & - \end{pmatrix}$$

If no unitary matrix can be found which will express the representation

$[r_{mn}]$ as the direct sum of small matrices of lower order, then $[r_{mn}]$ has been completely reduced by the particular choice of $\psi_1 \psi_2 \dots \psi_s$. The same choice will also completely reduce the representations of the other rotations of $G(\underline{k})$.

The small matrices are called the irreducible representations of $G(\underline{k})$. Under $[r_{mn}]$ the transformation of, for example, ψ_2 and ψ_3 , will be governed only by the 2-dimensional irreducible representation

$$\begin{bmatrix} b_{11} & b_{12} \\ b_{21} & b_{22} \end{bmatrix}$$

so that they transform into each other or into degenerate linear combinations of each other, but not into any of the (s-2) other wave functions.

This will be the case for any other rotation r in $G(\underline{k})$, ψ_2 and ψ_3 will always be the wave functions of a doubly-degenerate irreducible representation associated with one of the energy eigenfunctions of the point \underline{k} .

It may be shown (cf. Eyring, Walter and Kimball p.183) that there will be as many irreducible representations as there are classes of the group. This fact is of value in finding the dimensions of the representations. All the wave functions at \underline{k} can thus be classified under the various irreducible representations by which their transformations under the symmetry operations of the group $G(\underline{k})$ are determined.

The Character Table.

This can be calculated from the group multiplication table without a knowledge of the irreducible representations, or their wave functions (cf. Margenau and Murphy p.535), and it gives the

character (or trace) of all the irreducible representations of the group. The character of a particular operation, which is the same for all members of a class, and which is invariant under unitary transformations, shows how the wave functions transform under the irreducible representation to which they belong.

For example, if there is only one wave function belonging to an irreducible representation, this can only transform into itself or into $(-1) \times$ itself. The small matrices to which it belongs will all be one-dimensional with characters ± 1 . If, on the other hand, the level is n -fold degenerate, a wave function may transform into any of the n wave functions of the level and the irreducible representation will be n -dimensional. Since the identity transformation, $r=E$, is always a unit matrix, its character gives the dimension of the representation.

It may be shown (cf. Eyring, Walter and Kimball p.181) that the sum of the squares of the dimensions of the irreducible representations of a group is equal to the order g of the group

$$g = n_1^2 + n_2^2 + \dots + n_n^2 \quad (2)$$

where n is the number of irreducible representations, or the number of classes of the group.

The character tables of symmetry points of the Brillouin Zones of body centred cubic and face centred cubic crystals have been given by Bouckaert, Smoluchowski and Wigner (1936).

The Irreducible Representations of the Point $W(\frac{\pi}{a}(1,2,0))$.

The Brillouin Zone is shown with the three points equivalent to \underline{k} marked. Together with W itself, these are

$$\underline{k} = \frac{\pi}{a} (1,2,0)$$

$$\underline{k} = \frac{\pi}{a} (1,-2,0)$$

$$\underline{k} = \frac{\pi}{a} (-1,0,-2)$$

$$|K_m| = \frac{4\pi}{a}$$

$$|K_n| = \frac{2\pi\sqrt{3}}{a}$$

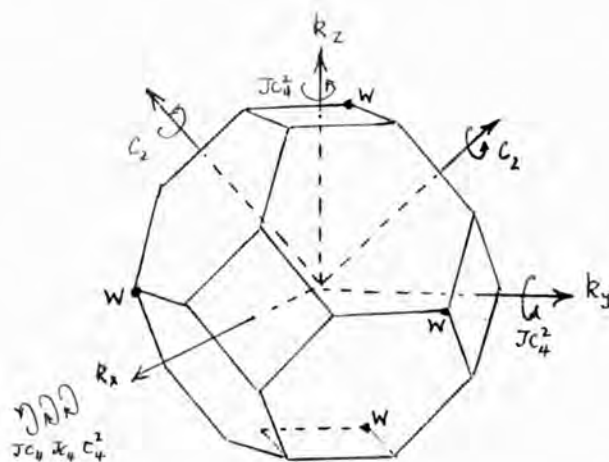


Fig. 3. The group $G(\underline{k})$ of W .

By permutation of the co-ordinates of \underline{k} , the elements of $G(\underline{k})$ are seen to be

$$\begin{aligned}
 E &= \begin{pmatrix} x & y & z \\ x & y & z \end{pmatrix} \\
 C_4^2 &= \begin{pmatrix} x & y & z \\ x & -z & +y \end{pmatrix} \\
 C_2 &= \begin{pmatrix} x & y & z \\ -x-z & -y & \end{pmatrix} \quad \text{and} \quad \begin{pmatrix} x & y & z \\ -x & z & y \end{pmatrix} \\
 JC_4 &= \begin{pmatrix} x & y & z \\ -x & z & -y \end{pmatrix} \quad \text{and} \quad \begin{pmatrix} x & y & z \\ -x-z & & y \end{pmatrix}
 \end{aligned} \tag{3}$$

$$JC_4^2 = \begin{pmatrix} x & y & z \\ x & y & -z \end{pmatrix} \text{ and } \begin{pmatrix} x & y & z \\ x & -y & z \end{pmatrix}$$

falling into five classes.

Since the order of the group is eight and there are five classes, equation (2) becomes for E

$$8 = n_1^2 + n_2^2 + n_3^2 + n_4^2 + n_5^2$$

which has the unique solution

$$8 = 1^2 + 1^2 + 1^2 + 1^2 + 2^2$$

There are therefore 5 irreducible representations at W, of which four correspond to single energy levels and the fifth to a doubly-degenerate level. In the notation of Howarth and Jones these are $W_s, W_p^1, W_d, W_f, W_p^2$.

Table 3 is the character table. (Bouckaert, Smoluchowski and Wigner, 1936)

| | E | C_4^2 | C_2 | JC_4 | JC_4^2 |
|---------|---|---------|-------|--------|----------|
| W_s | 1 | 1 | 1 | 1 | 1 |
| W_p^1 | 1 | 1 | -1 | -1 | 1 |
| W_d | 1 | 1 | 1 | -1 | -1 |
| W_f | 1 | 1 | -1 | 1 | -1 |
| W_p^2 | 2 | -2 | 0 | 0 | 0 |

Table 3. The Character Table of $W(\frac{\pi}{a}(1,2,0))$.

The Wave Function at W_2^1 .

Choosing the x axis as polar axis and measuring φ w.r.t. the $z = 0$ plane, transform C_4^2 , JC_4 and JC_4^2 into polar co-ordinates, taking, for example, the first operation of the pair in the case of the second and third operations.

$$C_4^2 = \begin{pmatrix} \theta & \varphi \\ \theta & \varphi + \pi \end{pmatrix} \quad JC_4 = \begin{pmatrix} \theta & \varphi \\ \pi - \theta & \varphi - \frac{\pi}{2} \end{pmatrix} \quad JC_4^2 = \begin{pmatrix} \theta & \varphi \\ \theta & -\varphi \end{pmatrix} \quad (4)$$

Under JC_4^2 $\psi \rightarrow \psi$, from the character table for W_2^1 .

Since the wave function may be written

$$\begin{aligned} \psi &= \sum (A_{lm} \cos m\varphi + B_{lm} \sin m\varphi) Y_l^m(\cos \theta) R_l(r) \\ &\rightarrow \sum (A_{lm} \cos m\varphi - B_{lm} \sin m\varphi) Y_l^m(\cos \theta) R_l(r) \end{aligned} \quad (5)$$

for all A_{lm} , B_{lm} ,

$$B_{lm} = 0 \quad (6)$$

for all l and m , and $\sin m\varphi$ terms vanish throughout the expansion.

Under C_4^2 , $\psi \rightarrow \psi$

$$\sum A_{lm} \cos m(\varphi + \pi) Y_l^m(\cos \theta) R_l(r) = \sum A_{lm} \cos(m\varphi) Y_l^m(\cos \theta) R_l(r)$$

Hence

$$m = \text{even.} \quad (7)$$

Under JC_4 , $\psi \rightarrow -\psi$

$$\sum A_{lm} \cos m\varphi \cos \frac{\pi}{2} Y_l^m(-\cos \theta) R_l(r) = \sum A_{lm} \cos m\varphi Y_l^m(\cos \theta) R_l(r)$$

the sine terms vanishing on the L.H.S. since $\sin \frac{m\pi}{2} = 0$, m even.

Hence if

$$\begin{aligned}
 m = 0, 4, 8 \dots & & m + l = \text{odd, or } l = \text{odd} \\
 m = 2, 6, 10 \dots & & m + l = \text{even, or } l = \text{even}
 \end{aligned}
 \tag{8}$$

When the conditions (6) and (7) and (8) are applied to the wave function (5), most of the terms vanish. The remaining terms, up to $l = h$, are

$$\begin{aligned}
 \psi_{W_P} = & A_{10} Y_1^0(\cos\theta) R_1(r) + A_{22} \cos 2\varphi Y_2^2(\cos\theta) R_2(r) \\
 & + A_{30} Y_3^0(\cos\theta) R_3(r) + A_{42} \cos 2\varphi Y_4^2(\cos\theta) R_4(r) + \dots
 \end{aligned}
 \tag{9}$$

or, reverting to Cartesian co-ordinates, and writing ψ in its even and odd expansions

$$\begin{aligned}
 \psi_{W_P} = & \left[A \left(\frac{y^2 - z^2}{r^2} \right) R_2(r) + B \left(\frac{y^2 - z^2}{r^2} - \frac{6}{7} \left(\frac{y^2 - z^2}{r^2} \right) \right) R_4(r) \right] \\
 & + i \left[P \left(\frac{x}{r} \right) R_1(r) + Q \left(\frac{x^3}{r^3} - \frac{3}{5} \frac{x}{r} \right) R_3(r) \right]
 \end{aligned}
 \tag{10}$$

where A, B, P and Q are all real coefficients.

It is seen that these are the only four coefficients out of the original $\sum_{l=0}^4 (2l+1) = 25$ which remain in the expansion of the wave function when the symmetry restrictions are applied.

The Wave Function at W_P^2 .

This is a doubly-degenerate level, and examination of the elements of the group $G(\underline{k})$ in equations (3) shows that the degeneracy occurs in the y- and z-co-ordinates, and that the irreducible representations must be

$$\begin{aligned}
 W_P^2 & \quad E \quad C_4^2 \quad C_2 \quad JC_4 \quad JC_4^2 \\
 & \quad \begin{bmatrix} 1 & 0 \\ 0 & 1 \end{bmatrix} \quad \begin{bmatrix} -1 & 0 \\ 0 & -1 \end{bmatrix} \quad \begin{bmatrix} 0 & 1 \\ 1 & 0 \end{bmatrix} \quad \begin{bmatrix} 0 & 1 \\ -1 & 0 \end{bmatrix} \quad \begin{bmatrix} -1 & 0 \\ 0 & +1 \end{bmatrix}
 \end{aligned}$$

Let the degenerate wave functions be ψ_1 and ψ_2 . Any linear combination of these, $\psi = C_1\psi_1 + C_2\psi_2$ is a wave function of W_p^2 .

$$\begin{aligned} \psi &= C_1 \sum (A_{lm} \cos m\varphi + A'_{lm} \sin m\varphi) Y_l^m(\cos \theta) R_l(r) \\ &+ C_2 \sum (B'_{lm} \cos m\varphi + B_{lm} \sin m\varphi) Y_l^m(\cos \theta) R_l(r) \end{aligned}$$

Under the same transformations, which were applied for W_p^1 (equation (4)) we have:

Under $J C_4^2$

$$\begin{aligned} C_1\psi_1 + C_2\psi_2 &\rightarrow J C_4 (C_1\psi_1 + C_2\psi_2) \\ &= \begin{bmatrix} 1 & 0 \\ 0 & -1 \end{bmatrix} (C_1\psi_1 + C_2\psi_2) = (C_1\psi_1 - C_2\psi_2) \\ &= C_1 \sum (A_{lm} \cos m\varphi + A'_{lm} \sin m\varphi) Y_l^m(\cos \theta) R_l(r) \\ &\quad - C_2 \sum (B'_{lm} \cos m\varphi + B_{lm} \sin m\varphi) Y_l^m(\cos \theta) R_l(r) \\ &\rightarrow C_1 \sum (A_{lm} \cos m\varphi - A'_{lm} \sin m\varphi) Y_l^m(\cos \theta) R_l(r) \\ &\quad + C_2 \sum (B'_{lm} \cos m\varphi - B_{lm} \sin m\varphi) Y_l^m(\cos \theta) R_l(r) \end{aligned}$$

$$A_{lm}' = B_{lm}' = 0 \tag{11}$$

$$\psi_1 = \sum A_{lm} \cos m\varphi Y_l^m(\cos \theta) R_l(r) \tag{12}$$

$$\psi_2 = \sum B_{lm} \sin m\varphi Y_l^m(\cos \theta) R_l(r)$$

Under C_4^2

$$(C_1\psi_1 + C_2\psi_2) \rightarrow - (C_1\psi_1 + C_2\psi_2)$$

$$\begin{aligned}
 & -(C_1 \sum A_{lm} \cos m\varphi - C_2 \sum B_{lm} \sin m\varphi) Y_l^m(\cos \theta) R_l(r) \\
 & \rightarrow (C_1 \sum A_{lm} (\cos m\varphi \cos m\pi - \sin m\varphi \sin m\pi) \\
 & \quad + C_2 \sum B_{lm} (\sin m\varphi \cos m\pi + \cos m\varphi \sin m\pi)) Y_l^m(\cos \theta) R_l(r)
 \end{aligned}$$

Hence

$$m = \text{odd.} \quad (13)$$

Under $J C_4$.

$$\begin{aligned}
 & (C_1 \psi_1 + C_2 \psi_2) \rightarrow (C_2 \psi_1 - C_1 \psi_2) \\
 & (C_2 \sum A_{lm} \cos m\varphi - C_1 \sum B_{lm} \sin m\varphi) Y_l^m(\cos \theta) R_l(r) \\
 & \rightarrow (C_1 \sum A_{lm} (\cos m\varphi \cos \frac{m\pi}{2} + \sin m\varphi \sin \frac{m\pi}{2}) \\
 & \quad + C_2 \sum B_{lm} (\sin m\varphi \cos \frac{m\pi}{2} - \sin \frac{m\pi}{2} \cos m\varphi)) Y_l^m(\cos \theta) R_l(r)
 \end{aligned}$$

Since this is true for all C_1, C_2

$$A_{lm} = B_{lm} \sin \frac{m\pi}{2} (-1)^{l+m} \quad (14)$$

Hence by (11), (13) and (14)

$$\begin{aligned}
 \psi_1 = & A_{11} \cos \varphi Y_1^1(\cos \theta) R_1(r) + A_{21} (\cos \varphi) Y_2^1(\cos \theta) R_2(r) \\
 & + A_{31} \cos \varphi Y_3^1(\cos \theta) R_3(r) + A_{33} \cos 3\varphi Y_3^3(\cos \theta) R_3(r) \\
 & + A_{41} \cos \varphi Y_4^1(\cos \theta) R_4(r) + A_{43} \cos 3\varphi Y_4^3(\cos \theta) R_4(r) \quad (15)
 \end{aligned}$$

with an equivalent expression in sine terms for ψ_2 .

In Cartesian co-ordinates, one of the degenerate pair at W_p^2 (ψ_1) is

$$\psi_{W_p^2} = \left[A \left(\frac{xy}{r^2} \right) R_2(r) + B \left(\frac{z^2 xy}{r^4} - \frac{1}{7} \frac{x y}{r^2} \right) R_4(r) + C \left(\frac{x^2 - y^2}{r^4} \right) xy R_4(r) \right] \\ + i \left[P \left(\frac{y}{r} \right) R_1(r) + Q \left(\frac{y^3}{r^3} - \frac{3}{5} \frac{y}{r} \right) R_3(r) + S \left(\frac{(z^2 - x^2)y}{r^3} \right) R_3(r) \right]$$

and the other will, of course, give the same energy.

Calculations were carried out for W_p^1 and W_p^2 , since, according to Heine's results, these are the two representations of the lowest energy at W.

From the expression for ψ_1 in polar co-ordinates (eq.(15)) it is seen that the function vanishes over the $\phi = \pi/2$ plane ($y=0$ plane). It therefore possesses behavior similar to that of an atomic p-function with a single nodal plane through the origin. Its degenerate partner also possesses p-like behavior, with a nodal plane at $\phi = 0$.

The notation 'p-like' is not so satisfactory for the wave function at W_p^1 , for although the odd terms of the expansion vanish over the whole plane $\theta = \pi/2$ the even terms do not vanish except in the planes $\phi = \pm \frac{\pi}{4}$. The wave function possesses a single node through the origin, but it lies along the lines of intersection of these two planes, rather than being a plane node, as it is in the atomic function.

The Wave Function at Γ .

The analysis is identical with that for the point W. The group $G(\underline{k})$ is the full rotation group $G(\underline{R})$. It has ten irreducible representations with the lowest energy in aluminium occurring for a singlet s-state Γ_s , which also has the full symmetry of the lattice. The wave function is found to be

$$\begin{aligned} \psi_s = & A R_0(r) + A_4 \left\{ Y_4^0(\cos \theta) + \frac{1}{168} \cos 4\phi Y_4^4(\cos \theta) \right\} R_4(r) \\ & + A_6 \left\{ Y_6^0(\cos \theta) - \frac{1}{360} \sin 2\phi Y_6^4(\cos \theta) \right\} R_6(r) \end{aligned}$$

or, in Cartesian co-ordinates.

$$\psi_s = A R_0(r) + B \left(\frac{x^4 + y^4 + z^4}{r^4} - \frac{3}{5} \right) R_4(r) + C \left(\frac{x^2 y^2 z^2}{r^6} + \frac{1}{22} \left(\frac{x^4 + y^4 + z^4}{r^4} - \frac{3}{5} \right) - \frac{1}{105} \right) R_6(r).$$

Chapter VI. The Potential in the Atomic Cell.

One of the chief difficulties involved in any band structure calculation is the accurate determination of the form of the potential $V(r)$ in the Schrodinger equation. In the cellular method, this affects the wave function through the radial functions $R_l(r)$ which are the solutions of equation 5 (Ch.IV).

In aiming at an accuracy of the order of 0.01 Ry in the final energy levels, Heine has made a careful determination of $V(r)$ for aluminium, taking into consideration all the factors which will affect the potential distribution in the neighbourhood of a conduction electron. These factors fall into two classes; those arising from the ion-core potential, and those arising from the distribution of all the other conduction electrons.

The Ion-Core Potential.

A self-consistent Hartree-Fock potential was available (Froese 1957) for aluminium.

It was estimated that a small potential arising from correlation between ion-core electrons could not affect the energy by more than 0.01 Ry. The error involved in calculating this potential from the redistribution of charge density on account of correlation between electrons in the ion cores of sodium (atomic number, $Z = 11$) for which calculations were available, instead of in those of aluminium ($Z = 13$) was therefore negligible.

A large contribution to the potential results from exchange between the ion-core electrons and the conduction electrons. In the Hartree-Fock approximation, the exchange energy of the electrons may be expressed as an effective potential (Slater 1951).

$$-(V_{\text{ex}}(\underline{r}_1))_i = - \sum_{\alpha} \frac{\int \psi_{\alpha}^*(\underline{r}_2) \psi_{\alpha}(\underline{r}_1) \frac{1}{r_{12}} \psi_i(\underline{r}_2) dV}{\psi_i(\underline{r}_1)} \quad (1)$$

acting upon an electron in state ψ_2 , by exchange with all electrons, α , of like spin. The contribution to the ion-core potential will be found by allowing the summation \sum_{α} to extend over the ion-core electrons only.

At points of high symmetry in the zone, the conduction electron wave function ψ_i often has predominantly atomic s-like, or predominantly atomic p-type symmetry near the nucleus (v.p.34). If V_{ex} is calculated using each of these atomic wave functions in turn, there is only a small difference in the resulting potentials except in a region very near the nucleus, where V_{ex} is, in any case, small in comparison with the ion-core potential. The error which will be involved in V_{ex} by neglecting terms in ψ_i with higher values of l will thus be negligible.

Near the nodes of the ψ_i , the denominator in equation 1 vanishes and V_{ex} undergoes wide fluctuations. Heine estimates that smoothing these out over a small range of r does not introduce an appreciable error into $E(\underline{k})$, but this seems questionable.

The correlation energy is a function of the whole system of electrons which cannot be split up into contributions from ion-core electrons and conduction electrons. Its effect will be discussed below.

Spin-orbit coupling in the ion cores will be negligible (0.003 Ry).

The Potential due to the Conduction Electrons.

As a first approximation, the potential due to the charge distribution of the conduction electrons may be calculated for atomic spheres (radius r_s) instead of for atomic polyhedra.

Using single wave functions $\psi_{\underline{k}}$ obtained from a preliminary calculation with an approximate potential, Heine calculate the charge density, $\rho(\underline{r}, \underline{k})$, assumed spherically symmetrical, of electrons in state \underline{k} at a large number of values of r up to r_s . This was done at a number of values of $|\underline{k}|$ spaced at equal intervals of $(|\underline{k}|^2)$ between $R = 0$ and the Fermi surface, and the results were integrated to give the charge density distribution $\rho(r)$, and hence the potential $V_c(r)$ arising from the whole Fermi distribution of conduction electrons.

The final self-consistent results showed that although the final wave functions differed by as much as 30% from those $\psi_{\underline{k}}$ assumed in calculating $V_c(r)$, (this was primarily the result of omitting the exchange potential V_{ex} from the calculation of the $\psi_{\underline{k}}$) $V_c(r)$ itself was very close to its self-consistent value.

Atomic Spheres Correction.

The calculation of the conduction electron potential which was discussed in the previous paragraph is only an approximation. In an accurate calculation the system cannot adequately be described as a system of overlapping spheres (fig.1) outside of which the charge density and the potential fall to zero. Such a description assumes a charge density which is too high in the regions, A, half-way between the atomic nuclei, and correspondingly low in the regions, B.

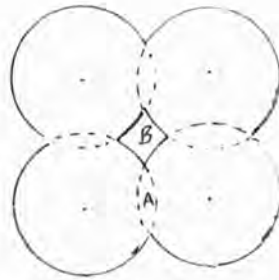


Fig. 1. Atomic spheres approximation.

The correction to be applied amounts to about 5% of the conduction electron potential. To find it, Heine considers the simple case of a face centred cubic lattice of protons with the lattice constant of aluminium and with a uniform distribution of electrons of density one electron per atom.

The atomic spheres calculation in this case is simply the Wigner-Seitz problem, with protons replacing the ion cores of sodium. The potential distribution $V(r)$ inside the atomic sphere of radius r_s is (Mott and Jones p.138)

$$V(r) = \frac{2}{r} - \frac{3}{r_s} - \frac{r^2}{r_s^3}$$

or, at a general point in the lattice

$$U(r) = \sum_i V(|r - r_i|)$$

The true electrostatic potential $U'(r)$ at a general point in this simple system may be calculated by the Ewald technique (cf. Kittel p.347). $U'(r)$ may also be expressed in terms of a sum of spherically symmetrical potentials

$$U'(r) = \sum_j V'(|r - r_j|)$$

Around any lattice point, therefore, there is a small, spherically symmetrical, correcting potential ΔV , given by

$$\sum_i \Delta V(r - r_i) = \Delta U = U'(r) - U(r)$$

In the i th cell, the distribution ΔV may be calculated by interpolation between a few points, r , for which $U'(r)$ has been determined. Thus, a corrected charge distribution in the cell, corresponding to a potential distribution $V + \Delta V$ may be found.

These results have been worked out for a uniform distribution of negative charge throughout the atomic sphere. They must be multiplied by a factor (in the case of aluminium 1.154) to allow for the fact that the conduction electron charge density is not constant throughout the sphere but is larger near $r \approx r_s$ than it is near the ion cores, and also by a factor 3 since aluminium has 3 valence electrons per atom.

Exchange and Correlation between the Conduction Electrons.

Since the electrons in aluminium are almost free, their interactions will approximate closely to the free electron behavior of the Bohn and Pines theory (Pines 1955).

The interaction Hamiltonian may be divided into two parts. There is a long-range contribution describing long-range Coulomb interactions which give rise to collective oscillations of the electron plasma. The excitation energy of these oscillations is large, so that they exist only in their ground states and do not affect the band width.

The other contribution is a short-range component $H_{s.r.}$ which governs the exchange energy of the electron gas and the remaining Coulomb interaction. The spherically symmetrical exchange potential $V_{ex}(\underline{k}, \underline{r})$ may be calculated by substituting $H_{s.r.}$ into Slater's equation (eq.(1)). Assuming the electron wave functions to be plane waves gives a potential

$$V_{\text{ex}}(\underline{k}) = 0.297 \left[2 - 4\beta + \frac{1-t^2}{t} \ln \frac{1+t}{1-t} \right] \text{ Ry.} \quad 0 \leq t \leq 1-\beta$$

$$= 0.297 \left[1 - 2\beta + \frac{\beta^2 + 3t^2 - 1}{2t} + \frac{1-t^2}{t} \ln \frac{1+t}{\beta} \right] \text{ Ry.} \quad 1-\beta \leq t \leq 1$$

where $t = 1.077|\underline{k}|$ and $\beta = 0.53$. This is independent of \underline{r} and may simply be added as a constant term to the energy of any state \underline{k} .

A term $\Delta V_{\text{ex}}(\underline{k}, \underline{r})$ taking account of the local variations of the electron density and calculated for a value of \underline{k} near the Fermi level \underline{k}_m was included in the total potential. This was a small term and its variation for \underline{k} introduced a negligible error into states not near \underline{k}_m .

In Heine's calculation the short range Coulombic correlation for all the electrons and also a small additional long-range Coulombic term not included in the plasma oscillation, were neglected in calculating the potential although their combined effect upon the band width was estimated to be about 0.03 Ry.

The Radial Integration.

The total crystal potential $V(r)$ is given by Heine at a rather small number of values of the radius r , throughout the atomic cell. This was interpolated using a 4-point Lagrangian interpolation formula, except in the region of r where the exchange term fluctuated so rapidly that a graphical interpolation seemed preferable. In view of the uncertainty in $V(r)$ at intermediate values of r , only four significant figures were retained in the radial integration and throughout the subsequent calculation.

The deviations of this interpolated potential from a more detailed table of Heine's actual potential which was later obtained* were small and probably did not introduce an error of more than

0.01 Ry. into $E(\underline{k})$.

Tables of the potential which was used are given in the appendix (pp. xv - xvi).

* I am indebted to Dr. V. Heine for making details of his calculation available to me.

Chapter VII. Numerical Calculation and Results.

The Surface Integration.

A surface integration over a $\frac{1}{2}$ -face of the atomic cell of any product $\frac{udv}{dn}$ etc. performed by covering the face by a rectangular network of thirteen points.

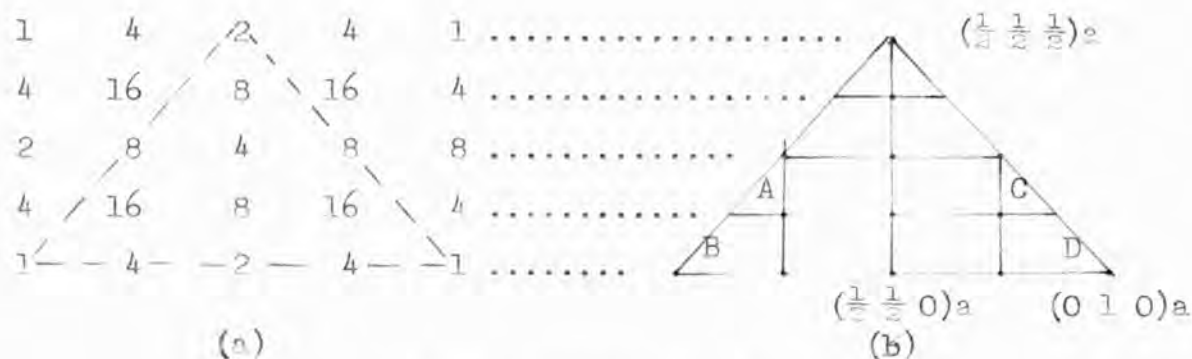


Fig. 1. Surface Integration Formula.

illustrated in fig.1 (b) for a $\frac{1}{2}$ -face parallel with the z-axis, and applying the cubature formula (Fig.1.(a)) given by Buckingham (p.497) to the values of $u \frac{dv}{dn}$ evaluated at the chosen points.

Such a procedure is equivalent to evaluating the integral of $u \frac{dv}{dn}$ over a strip AC taken in the surface by passing some simple curve through the points (cf. Buckingham p.78), and then performing a similar integration to sum the strips AC, BD etc. occurring in the surface.

The elements of the cubature formula are equivalent to the weighting factors which are applied to any given point on the surface in the conventional point matching procedure (v. Kohn 1952).

The Energy at Γ_3 .

The calculation to find the energy at this point will be described in some detail.

Since the point $k = 0$ in the Brillouin Zone has the full 48 symmetry of the cubic group, it is necessary to satisfy the boundary conditions on only a single $\frac{1}{4}$ -face of the surface of the atomic cell. All other faces will be equivalent to this one by symmetry. Consider for example a $\frac{1}{4}$ -face parallel to the z-axis such as that shown in fig. 2(a)

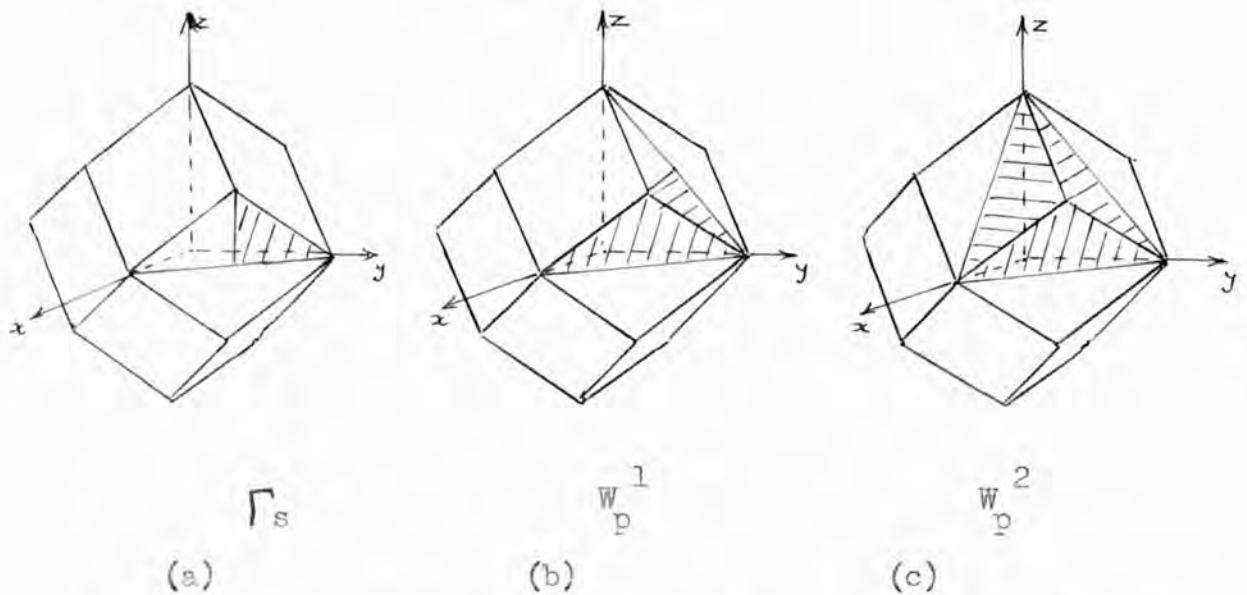


Fig. 2. Non-Equivalent surfaces in the Surface Integration.

The variational principle at $\underline{k} = 0$ is

$$\delta J = \delta \operatorname{Re} \int_{\frac{1}{4} \text{ z-face}} \psi^*(\underline{r}') \nabla_n \psi(\underline{r}) \exp(i\mathbf{k} \cdot \underline{\mathbf{r}}) dS.$$

$$\psi(\underline{r}) = AR_0(r) + B\left(\frac{x^4+y^4+z^4}{r^4} - \frac{3}{5}\right)R_4(r) + C\left(\frac{x^2y^2z^2}{r^6} + \frac{1}{22}\left(\frac{x^4+y^4+z^4}{r^4} - \frac{3}{5}\right) - \frac{1}{105}\right)R_6(r) \quad (1)$$

$$= \psi^*(r)$$

since $\psi(r)$ is real

$$= \psi^*(r')$$

since on translation to the conjugate face

$$\begin{pmatrix} r \\ r' \end{pmatrix} = \begin{pmatrix} x & y & z \\ -y & -x & z \end{pmatrix} = \begin{pmatrix} \psi(r) \\ \psi(r') \end{pmatrix} \quad (2)$$

Hence

$$\delta J = \delta \int_S \psi(r) \nabla_n \psi(r) dS$$

If $P_\ell = rR_\ell$

$$\begin{aligned} \nabla_n \psi &= \frac{x+y}{r^2} \left\{ A \left(\frac{\partial P_\ell}{\partial r} - \frac{P_\ell}{r} \right) + B \left(\frac{x+y+z}{r^4} - \frac{3}{5} \right) \left(\frac{\partial P_\ell}{\partial r} - \frac{P_\ell}{r} \right) \right. \\ &\quad \left. + C \left(\frac{x^2 y^2 z^2}{r^6} + \frac{1}{22} \left(\frac{x+y+z}{r^4} - \frac{3}{5} \right) - \frac{1}{105} \right) \left(\frac{\partial P_\ell}{\partial r} - \frac{P_\ell}{r} \right) - C \frac{4x^2 y^2 z^2 P_\ell}{r^6} \right\} \\ &\quad - \frac{4}{r^6} \left\{ \frac{P_\ell}{r} x(y+z) + B \frac{P_\ell}{r} y(x+z) + C \frac{P_\ell}{r} \frac{1}{22} x(y+z) + C \frac{P_\ell}{r} \frac{1}{22} y(x+z) \right\} \quad (3) \end{aligned}$$

The calculation of J then involves the substitution of equations (1) and (3) into (2) and the numerical calculation of the coefficients of each of the products A, B, C, AB, BC, AC at all values of $(r) = (x,y,z)$ required in the surface integration. For example, the expression to be evaluated for B is

$$\begin{aligned} B &= \left[\frac{P_\ell}{r} \left(\frac{x+y+z}{r^4} - \frac{3}{5} \right) \right] \left[\frac{x+y}{r^2} \left\{ \left(\frac{x+y+z}{r^4} - \frac{3}{5} \right) \left(\frac{\partial P_\ell}{\partial r} - \frac{P_\ell}{r} \right) - \frac{4P_\ell}{r} \left(\frac{x+y+z}{r^4} \right) \right. \right. \\ &\quad \left. \left. + \frac{4}{r} \left(\frac{P_\ell}{r} \frac{x+y}{r^3} \right) \right\} \right] \end{aligned}$$

for each of the nine points of the $\frac{1}{4}$ - face.

Full details of the calculation of these coefficients are given in the appendix.

Variation of J w.r.t. the parameters A, B, C , leads to three simultaneous linear equations in A, B and C which will be compatible only for a particular choice of the trial energy λ' used in the radial integration. In this case the determinant of the coefficients vanishes.

Table I. shows the values of the determinants which are obtained for three trial energies, λ' , when one, two and three terms respectively are used in the expansion of $\psi(r, \lambda')$. A graphical interpolation (fig. 3) shows that the energy vanishes at the energy shown in the fourth column.

| λ' (Ry) | -.637 | -.237 | -.037 | Energy at Γ_3 | Point Matching |
|-----------------|-------|-------|-------|----------------------|----------------|
| $l = 0$ | 1 | -.194 | -.372 | -.33 | - |
| $l = 0, 4$ | 1 | -.126 | -.184 | -.31 | -.35 |
| $l = 0, 4, 6$ | 1 | -.093 | -.126 | -.31 | -.34 |

Table I. Secular Determinants at Γ_3 .

The convergence is satisfactory, and compares well with a point matching calculation (cf. Howarth and Jones 1952), which was carried out for a large number of combinations of the same points that were considered in the surface integrations. The normal derivatives of $\psi(r, \lambda')$ which, for $k = 0$, are all that are required for point matching, had already been evaluated as an incidental part of the main calculation. The figures in the fifth column represent a very rough average of the results of the various combinations of points, the calculation being carried through more as a check on procedure than as an accurate comparison.

The normalised wave function in the ground state at $E = -0.31$ Ry.

$$\psi = 0.9997Y_0(\cos\theta)R_0(r) + 0.0240Y_4(\cos\theta)R_0(r) + 0.0003Y_6(\cos\theta)R_6(r) \quad (4)$$

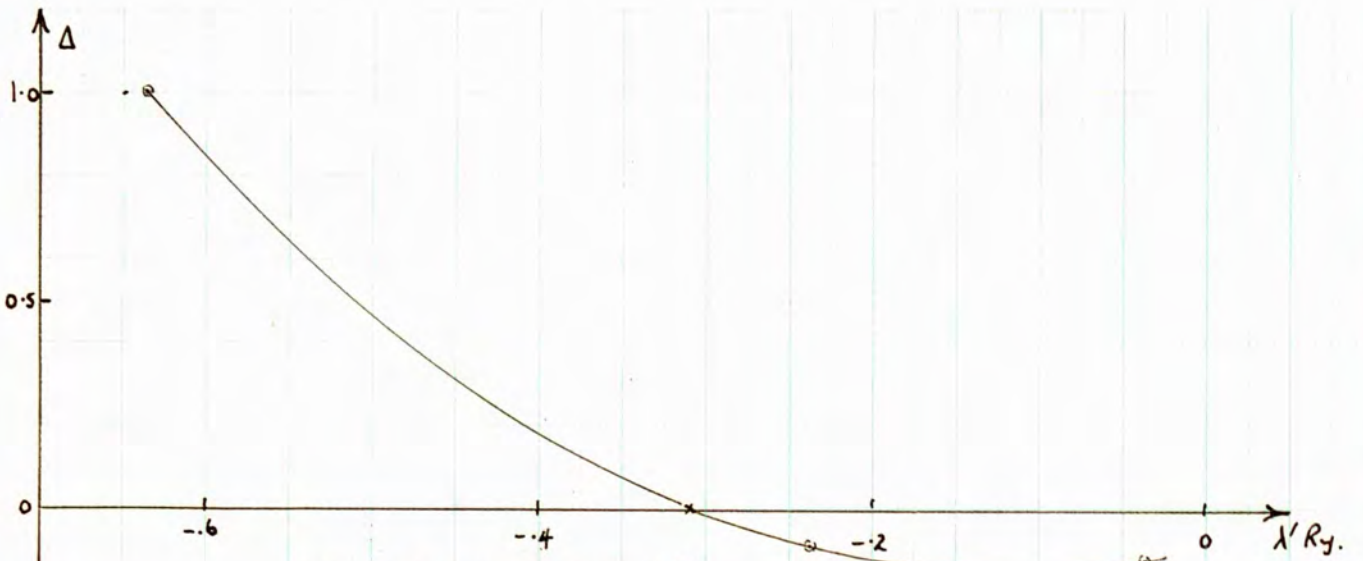


Fig 3. Secular Determinants, Δ , at W_5^1



Fig 4. Secular Determinants, Δ , at W_p^1

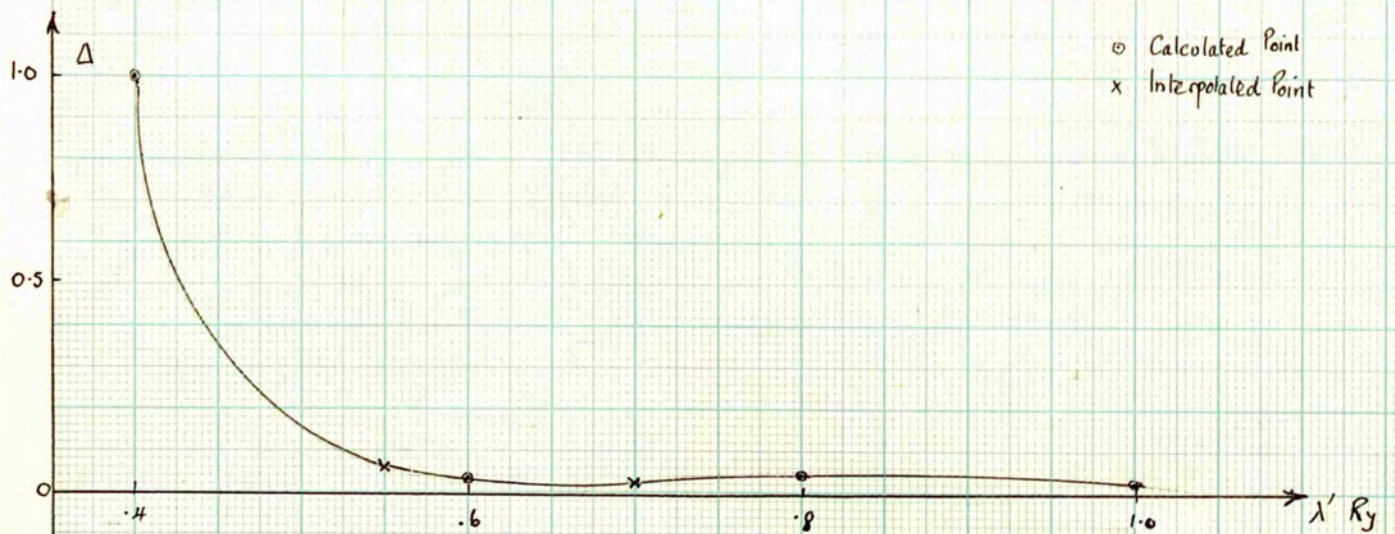


Fig 5. Secular Determinants, Δ , at W_p^2

○ Calculated Point
x Interpolated Point

The Energy at W.

The calculation of the levels at W is identical, but since the symmetry of W is much lower than that of Γ_5 , larger areas of the surface have to be considered. These are shown in Fig.1 (b) and (c) for the levels W_p^1 and W_p^2 respectively.

In addition, the labour is increased by the presence of odd as well as even spherical harmonics in the wave function, so that for expansions of $\psi(r, \lambda')$ up to $\lambda = 4$, the number of surface integrations required for a given trial energy increases from four at Γ_5 to fourteen at W_p^1 and to forty-eight at W_p^2 .

The final values of the determinants are shown in tables 2. and 3. and graphically in figs. 4 and 5.

| λ' (Ry.) | 0.4 | 0.6 | 0.8 | 1.0 | Lowest energy (Ry.) |
|------------------------|-----|---------|--------|--------|---------------------|
| $\lambda = 1, 2$ | 1 | -3.38 | -8.78 | -10.58 | 0.44 |
| $\lambda = 1, 2, 3$ | 1 | -1.040 | -1.740 | -0.880 | 0.48 |
| $\lambda = 1, 2, 3, 4$ | 1 | -0.0374 | 0.373 | 0.301 | 0.491 |

Table 2. Secular Determinants, W_p^1 .

| λ' (Ry.) | 0.4 | 0.6 | 0.8 | 1.0 | Lowest energy (Ry.) |
|------------------------|-----|--------|--------|-------|---------------------|
| $\lambda = 1, 2$ | 1 | 0.32 | 1.75 | 2.44 | - |
| $\lambda = 1, 2, 3$ | 1 | -0.352 | -0.075 | 0.048 | (0.42) |
| $\lambda = 1, 2, 3, 4$ | 1 | 0.035 | 0.027 | 0.015 | - |

Table 3. Secular Determinants, W_p^2 .

For the doubly-degenerate level W_p^2 , the final determinants do not vanish at any energy in the range 0.4 to 1.0 Ry. It seems likely therefore that for a wave function of this symmetry an expansion which includes spherical harmonics of order up to $\lambda = 4$ only, is not sufficient.

At W_P^1 , the lowest value of the energy at which the determinant vanishes converges satisfactorily. The normalised wave function is found to be almost entirely atomic p-like.

$$\psi = .0848Y_2(\cos\theta)R_2(r) - .0004Y_4(\cos\theta)R_4(r) - i\{1.0036Y_1(\cos\theta)R_1(r) - .0027Y_3(\cos\theta)R_3(r)\} \quad (5)$$

with energy 0.491 Ry.

When the correlation energy, V_{PP} , is included, this corresponds to an energy of 1.04 Ry. relative to the ground state. This is to be compared with Heine's value of 1.012 Ry.

The agreement between these values is better than could be expected in the light of the unsatisfactory result for W_P^2 . On the other hand, equation (5) indicates that the effect of spherical harmonics of order higher than $l = 4$ cannot be very great in the wave function at W_P^1 .

However, it is by no means certain that the lowest energy which appears in table 2. is the lowest energy occurring for a wave function with the symmetry of W_P^1 . Jenkins and Pincherle (1954) have shown that when, by suitable choice of the trial functions, the volume integral vanishes from the variational principle (eq.(10), p.14), trial functions which satisfy the equation

$$\psi(\underline{r}') = -\exp(i\underline{k} \cdot \underline{r})\psi(\underline{r})$$

as well as true Bloch functions governed by

$$\psi(\underline{r}') = +\exp(i\underline{k} \cdot \underline{r})\psi(\underline{r})$$

become possible and give rise to spurious roots in the secular equation.

In this case the root occurring at $\lambda' = 0.491$ may be a spurious root, and that occurring at 0.619 a true one. The normalised wave function at $\lambda' = 0.619$ is

$$\psi = .0858Y_2(\cos\theta)R_2(r) - .0013Y_4(\cos\theta)R_4(r) + i \left\{ 1.0036Y_1(\cos\theta)R_1(r) - .0122Y_3(\cos\theta)R_3(r) \right\} \quad (6)$$

which, again, is predominantly p-type so that there is no reason to prefer either root on the grounds of the symmetry of the wave function,

In the complete form of the variational principle, $\delta J = 0$, (eq. (11) p.21) for any trial energy, λ' , which is not the true energy λ , the volume integral becomes

$$\delta \int_{\Omega} \psi^* (H - \lambda) \psi d\omega = \delta \sum_i (\lambda' - \lambda) A_i^* A_i \quad (7)$$

for normalised trial functions given by equation (4) p.18.

Neglecting this term in δJ assumes that Schrodinger's equation is satisfied inside the atomic cell at the same energy, λ' , which minimises the surface integral. This becomes strictly true only when an infinite number of spherical harmonics is included in ψ . For a limited number of terms, the best value of λ will not, in general, be equal to the value λ' which appears in the best trial function, since in this case, the variational principle must effect a compromise between a mismatch at the cell boundaries and a poor solution of Schrodinger's equation throughout the cell.

Thus the determinantal equation which has been solved for λ is only an approximation (an approximation which improves as the

order of the surface harmonics in the expansion of ψ increases) to a latent root equation

$$0 = \delta J = \delta \sum_i (\lambda' - \lambda) A_i^* A_i + \delta \int_S \sum_{ij} A_i A_j Y_i(\cos \theta) R_i(r) \nabla_n (Y_j(\cos \theta) R_j(r)) \exp(i \underline{k} \cdot \underline{r}) dS \quad (8)$$

for all variations of the coefficients A_i together with the further condition

$$\partial J / \partial \lambda' = 0 \quad (9)$$

These equations will give no spurious solutions for the unknown parameters, A_i and λ' .

Jenkins (1954) has shown that the correct value of λ may be found from equation (8) without the necessity of finding, by trial, the solution which also satisfies equation (9) exactly. For it may be shown that when $\partial J / \partial \lambda'$ is zero $d\lambda / d\lambda'$ is also zero. Thus from the latent roots $(\lambda' - \lambda)$ of equation (8) for various trial energies λ' , graphs of λ vs λ' may be drawn which pass through a stationary point at the best value of λ .

Jenkins found this method satisfactory provided the latent roots could be calculated exactly. In the present calculations the method was applied to the ground-state energy Γ'_S . A trial function containing three spherical harmonics up to order $l = 6$ gave three latent roots. Two of these were very large in comparison with the lowest root governing the variation of the ground-state energy with λ' . Thus, although this root could be calculated accurately from any given latent-root equation, the surface integrations occurring in the equation could not be calculated with sufficient accuracy for the variation of λ which was obtained to have any numerical significance.

Since the lowest root at W_p^1 is of the same order of magnitude as that at Γ_s , and subject to the same uncertainty, the latent root calculation was not carried out for this energy level.

Apart, then, from the agreement of the lower value with the energy calculated by Heine by the O.P.W. method, these calculations lead to no means of preferring either of the lowest roots occurring at W_p^1 .

Conclusion.

The present calculations have not proved to be sufficiently exact to provide an adequate confirmation of Heine's results on the band structure of aluminium.

The difference between the interpolated potential used and Heine's potential cannot have introduced a discrepancy of more than 0.01 Ry., and the error involved in the surface integration formula is probably not greater than this. The interpolation of the secular determinants does not introduce an appreciable error, since the interpolation of the individual terms of the determinants which vary much more smoothly with energy than the determinants themselves may be carried out easily.

The remaining discrepancies must be due to the form of the trial wave functions. Although an expansion in spherical harmonics up to order $l = 4$ has been adequate for the wave function at W_{Γ}^1 it has been inadequate for the wave function at W_{Γ}^2 , where fourth order terms have a large effect upon the secular equation. Thus, even when the best possible matching conditions are used, the use of higher order terms in the wave function appears to be unavoidable.

A P P E N D I X.

- i. The calculation of the surface integrals.
- ii. Tables of crystal potential.

(i)

Calculation of $J = \int_S \psi(r) \nabla_n \psi(r) dS$ for Γ_S .

$$\psi(r) = \frac{AP_0}{r} + \frac{BP_4}{r} \left(\frac{x^4+y^4+z^4}{r^4} - \frac{3}{5} \right) + \frac{CP_6}{r} \left(\frac{x^4y^4z^4}{r^6} + \frac{1}{22} \left(\frac{x^4+y^4+z^4}{r^4} - \frac{3}{5} \right) - \frac{1}{105} \right)$$

For $\frac{z}{r}$ -face chosen parallel to z-axis

$$\begin{aligned} \nabla_n \psi &= (\text{const.}) \left(\frac{\partial \psi}{\partial x} + \frac{\partial \psi}{\partial y} \right) \\ &= (\text{const.}) \left\{ \frac{x+y}{r^2} \left[A \left(\frac{\partial P_0}{\partial r} - \frac{P_0}{r} \right) + B \left(\frac{x^4+y^4+z^4}{r^4} - \frac{3}{5} \right) \left(\frac{\partial P_4}{\partial r} - \frac{P_4}{r} \right) \right. \right. \\ &\quad \left. \left. + C \left(\frac{x^4y^4z^4}{r^6} + \frac{1}{22} \left(\frac{x^4+y^4+z^4}{r^4} - \frac{3}{5} \right) - \frac{1}{105} \right) \left(\frac{\partial P_6}{\partial r} - \frac{P_6}{r} \right) - C \frac{4x^2y^2z^2P_6}{r^6} \right] \right. \\ &\quad \left. - \frac{4}{r^6} \left[B \frac{P_4}{r} x(y^4+z^4) + B \frac{P_4}{r} y(x^4+z^4) + C \frac{P_6}{r} \frac{1}{22} x(y^4+z^4) + C \frac{P_6}{r} \frac{1}{22} y(x^4+z^4) \right] \right\} \end{aligned}$$

$$\text{Coefficient of } A^2 = \left[\frac{P_0}{r} \right] \left[\left(\frac{\partial P_0}{\partial r} - \frac{P_0}{r} \right) \frac{x+y}{r^2} \right]$$

$$\begin{aligned} \text{Coefficient of } B^2 &= \left[\frac{P_4}{r} \left(\frac{x^4+y^4+z^4}{r^4} - \frac{3}{5} \right) \right] \left[\frac{x+y}{r^2} \left(\frac{x^4+y^4+z^4}{r^4} - \frac{3}{5} \right) \left(\frac{\partial P_4}{\partial r} - \frac{P_4}{r} \right) \right. \\ &\quad \left. - \frac{4P_4}{r} \left(\frac{x^4+y^4+z^4}{r^4} \right) \right] + \frac{4}{r} \left[\frac{P_4}{r} \frac{x^4+y^4}{r^4} \right] \end{aligned}$$

$$\begin{aligned} \text{Coefficient of } C^2 &= \left[\frac{P_6}{r} \left(\frac{x^4y^4z^4}{r^6} + \frac{1}{22} \left(\frac{x^4+y^4+z^4}{r^4} - \frac{3}{5} \right) - \frac{1}{105} \right) \right] \\ &\quad \left[\frac{x+y}{r^2} \left(\frac{x^4y^4z^4}{r^6} + \frac{1}{22} \left(\frac{x^4+y^4+z^4}{r^4} - \frac{3}{5} \right) - \frac{1}{105} \right) \left(\frac{\partial P_6}{\partial r} - \frac{P_6}{r} \right) \right. \\ &\quad \left. - \left(6 \frac{x^2y^2z^2}{r^6} - 2 \frac{xyz^2}{r^4} + \frac{4}{22} \left(\frac{x^4+y^4+z^4}{r^4} \right) \frac{P_6}{r} \right) \right] + \frac{4}{22} \left[\frac{P_6}{r} \left(\frac{x^4+y^4}{r^4} \right) \right] \end{aligned}$$

(ii)

Writing the contributions to A^2 from $\psi(r)$ as $[A_1]$ and that from $\nabla_n \psi(r)$ as $[A_2]$ etc.

$$\text{Coefficient of AB} = [A_1][B_2] + [A_2][B_1]$$

$$\text{" " AC} = [A_1][C_2] + [A_2][C_1]$$

$$\text{" " BC} = [B_1][C_2] + [B_2][C_1]$$

Surface Integrations of Coefficients at \sqrt{s} .

| λ | A^2 | B^2 | C^2 | AB | AC | BC |
|-----------|---------|--------|--------|---------|--------|--------|
| -.037 | -.1480 | 2033.6 | 903.2 | - 2.118 | -5.084 | -407.7 |
| -.237 | -.0769 | 2662.5 | 1059.9 | + 2.921 | -3.812 | -392.7 |
| -.637 | +3.3978 | 4452.8 | 1376.1 | +23.051 | +3.143 | -282.5 |

(iii)

$$J = \int_S \psi(r') \nabla_n \psi(r) \exp(ik \cdot \underline{r}_t) dS \text{ for } W_D^1.$$

$$\psi(r) = u + iv$$

$$= \left[A \frac{P_r}{r} \left(\frac{y^2 - z^2}{r^2} \right) + B \frac{P_r}{r} \left(\frac{y^2 - z^2}{r^2} - \frac{6}{7} \frac{y^2 - z^2}{r^2} \right) \right] + i \left[P \frac{P_r}{r} \frac{x}{r} + Q \frac{P_r}{r} \left(\frac{x^2}{r^2} - \frac{2}{5} \frac{x}{r} \right) \right]$$

 $\nabla_n u(r)$, x-face*

$$\begin{aligned} & \frac{y+z}{r^2} \left\{ A \left(\frac{\partial P_r}{\partial r} - \frac{P_r}{r} \right) \left(\frac{y^2 - z^2}{r^2} \right) + B \left(\frac{\partial P_r}{\partial r} - \frac{P_r}{r} \right) \left(\frac{y^2 - z^2}{r^2} - \frac{6}{7} \frac{y^2 - z^2}{r^2} \right) - 2 \frac{y^2 - z^2}{r^2} \left(A \frac{P_r}{r} - \frac{6}{7} B \frac{P_r}{r} \right) - 4B \frac{P_r}{r} \frac{y^2 - z^2}{r^2} \right\} \\ & + 2 \left(A \frac{P_r}{r} - \frac{6}{7} B \frac{P_r}{r} \right) \frac{y-z}{r^2} + 4B \frac{P_r}{r} \frac{y^2 - z^2}{r^2} \end{aligned}$$

y-face

$$\begin{aligned} & \frac{y+z}{r^2} \left\{ A \left(\frac{\partial P_r}{\partial r} - \frac{P_r}{r} \right) \left(\frac{y^2 - z^2}{r^2} \right) + B \left(\frac{\partial P_r}{\partial r} - \frac{P_r}{r} \right) \left(\frac{y^2 - z^2}{r^2} - \frac{6}{7} \frac{y^2 - z^2}{r^2} \right) - 2 \frac{y^2 - z^2}{r^2} \left(A \frac{P_r}{r} - \frac{6}{7} B \frac{P_r}{r} \right) - 4B \frac{P_r}{r} \frac{y^2 - z^2}{r^2} \right\} \\ & + \left\{ 2 \left(A \frac{P_r}{r} - \frac{6}{7} B \frac{P_r}{r} \right) \frac{z}{r^2} + 4B \frac{P_r}{r} \frac{z^2}{r^2} \right\} \end{aligned}$$

 $\nabla_n v(r)$, x-face

$$\frac{y+z}{r^2} \left\{ P \left(\frac{\partial P_r}{\partial r} - \frac{P_r}{r} \right) \frac{x}{r} + Q \left(\frac{\partial P_r}{\partial r} - \frac{P_r}{r} \right) \left(\frac{x^2}{r^2} - \frac{2}{5} \frac{x}{r} \right) - \frac{x}{r} \left(P \frac{P_r}{r} + 3Q \frac{P_r}{r} \left(\frac{x^2}{r^2} - \frac{1}{5} \right) \right) \right\}$$

y-face

$$\begin{aligned} & \frac{y+z}{r^2} \left\{ P \left(\frac{\partial P_r}{\partial r} - \frac{P_r}{r} \right) \frac{x}{r} + Q \left(\frac{\partial P_r}{\partial r} - \frac{P_r}{r} \right) \left(\frac{x^2}{r^2} - \frac{2}{5} \frac{x}{r} \right) - \frac{x}{r} \left(P \frac{P_r}{r} + 3Q \frac{P_r}{r} \left(\frac{x^2}{r^2} - \frac{1}{5} \right) \right) \right\} \\ & + \frac{1}{r^2} \left\{ P \frac{P_r}{r} + 3Q \left(\frac{x^2}{r^2} - \frac{1}{5} \right) \right\} \end{aligned}$$

* x-face denotes a face parallel with the x-axis etc.

(iv)

For the x-face

$$\begin{aligned}\begin{pmatrix} \mathbf{r}' \\ \mathbf{r}' \end{pmatrix} &= \begin{pmatrix} x & y & z \\ x & -z & -y \end{pmatrix} = \begin{pmatrix} u & v \\ -u & v \end{pmatrix} \\ J &= \operatorname{Re} \int_S \psi^*(\mathbf{r}') \nabla_n \psi(\mathbf{r}) \exp(i\mathbf{k} \cdot \frac{\boldsymbol{\tau}}{r}) dS \\ &= \operatorname{Re} \int_S (-u-iv) \nabla_n (u+iv) \exp(-i\pi) dS \\ &= \int_S u(\mathbf{r}) \nabla_n u(\mathbf{r}) dS - \int_S v(\mathbf{r}) \nabla_n v(\mathbf{r}) dS\end{aligned}$$

For the y-face

$$\begin{aligned}\begin{pmatrix} \mathbf{r}' \\ \mathbf{r}' \end{pmatrix} &= \begin{pmatrix} x & y & z \\ -z & y & -x \end{pmatrix} \\ J &= \operatorname{Re} \int_S \psi^*(\mathbf{r}') \nabla_n \psi(\mathbf{r}) \exp(-\frac{\pi}{2} i) dS \\ &= \int_S u(\mathbf{r}') \nabla_n v(\mathbf{r}) dS - \int_S v(\mathbf{r}') \nabla_n u(\mathbf{r}) dS\end{aligned}$$

(u and v are evaluated on the conjugate face by making the substitution

$$\begin{pmatrix} \mathbf{r}' \\ \mathbf{r}' \end{pmatrix} = \begin{pmatrix} x & y & z \\ -z & y & -x \end{pmatrix}$$

(v)

W_P¹, x-face u(r)∇_nu(r)

$$\text{Coefficient of } A^2 \left[\frac{P_2}{r} \frac{y^2-z^2}{r^2} \left[\frac{y+z}{r^2} \left\{ \left(\frac{\partial P_2}{\partial r} - \frac{P_2}{r} \right) \frac{y^2-z^2}{r^2} - 2 \frac{P_2}{r} \left(\frac{y^2-z^2}{r^2} - \frac{y-z}{y+z} \right) \right\} \right] \right]$$

$$\text{Coefficient of } B^2 \left[\frac{P_2}{r} \left(\frac{y^2-z^2}{r^4} - \frac{6}{7} \frac{y^2-z^2}{r^2} \right) \left[\frac{y+z}{r^2} \left\{ \left(\frac{\partial P_2}{\partial r} - \frac{P_2}{r} \right) \left(\frac{y^2-z^2}{r^4} - \frac{6}{7} \frac{y^2-z^2}{r^2} \right) \right. \right. \right. \\ \left. \left. \left. + 2 \frac{P_2}{r} \left(\frac{6}{7} \frac{y^2-z^2}{r^2} - 2 \frac{y^2-z^2}{r^4} - \frac{6}{7} \frac{y-z}{y+z} + 2 \frac{y^2-z^2}{r^4(y+z)} \right) \right\} \right] \right]$$

$$\text{Coefficient of } AB \left[A_1 \right] \left[B_2 \right] + \left[A_2 \right] \left[B_1 \right]$$

x-face v(r)∇_nv(r)

$$\text{Coefficient of } P^2 \left[\frac{P_1}{r} \frac{x}{r} \left[\frac{y+z}{r^2} \left\{ \left(\frac{\partial P_1}{\partial r} - \frac{P_1}{r} \right) \frac{x}{r} - \frac{x}{r} \frac{P_1}{r} \right\} \right] \right]$$

$$\text{Coefficient of } Q^2 \left[\frac{P_1}{r} \frac{x}{r} \left(\frac{x^2}{r^2} - \frac{2}{5} \right) \left[\frac{y+z}{r^2} \frac{x}{r} \left\{ \left(\frac{\partial P_1}{\partial r} - \frac{P_1}{r} \right) \left(\frac{x^2}{r^2} - \frac{2}{5} \right) - 2 \frac{P_1}{r} \left(\frac{x^2}{r^2} - \frac{1}{5} \right) \right\} \right] \right]$$

$$\text{Coefficient of } PQ \left[P_1 \right] \left[Q_2 \right] + \left[P_2 \right] \left[Q_1 \right]$$

y-face v(r')∇_nu(r)

$$\text{Coefficient of } [A_2] \left[\frac{x+z}{r^2} \left\{ \left(\frac{\partial P_2}{\partial r} - \frac{P_2}{r} \right) \frac{y^2-z^2}{r^2} - 2 \frac{P_2}{r} \left(\frac{y^2-z^2}{r^2} - \frac{z}{x+z} \right) \right\} \right]$$

$$\text{Coefficient of } [B_2] \left[\frac{x+z}{r^2} \left\{ \left(\frac{\partial P_2}{\partial r} - \frac{P_2}{r} \right) \left(\frac{y^2-z^2}{r^4} - \frac{6}{7} \frac{y^2-z^2}{r^2} \right) \right. \right. \\ \left. \left. + 2 \frac{P_2}{r} \left(\frac{6}{7} \frac{y^2-z^2}{r^2} + \frac{6}{7} \frac{z}{x+z} - 2 \frac{y^2-z^2}{r^4} - \frac{z^2}{r^2(x+z)} \right) \right\} \right]$$

$$\text{Coefficient of } [P_1] \left[- \frac{P_1}{r} \frac{z}{r} \right]$$

$$\text{Coefficient of } [Q_1] \left[- \frac{P_1}{r} \frac{z}{r} \left(\frac{z^2}{r^2} - \frac{2}{5} \right) \right]$$

y-face u(r')∇_nv(r)

$$\text{Coefficient of } [A_1] \left[\frac{P_1}{r} \frac{y^2-z^2}{r^2} \right]$$

$$\text{Coefficient of } [B_1] \left[\frac{P_1}{r} \left(\frac{y^2-z^2}{r^4} - \frac{6}{7} \frac{y^2-z^2}{r^2} \right) \right]$$

(vi)

$$\text{Coefficient of } [P_2] \left[\frac{x+z}{r^2} \frac{x}{r} \left\{ \left(\frac{\partial P}{\partial r} - \frac{P}{r} \right) - \frac{P}{r} \left(1 - \frac{r^2}{x(x+z)} \right) \right\} \right]$$

$$\text{Coefficient of } [Q_2] \left[\frac{x+z}{r^2} \frac{x}{r} \left\{ \left(\frac{\partial P}{\partial r} - \frac{P}{r} \right) \left(\frac{x^2}{r^2} - \frac{2}{5} \right) - \frac{P}{r} \left(\frac{x^2}{r^2} - \frac{1}{5} \right) \left(1 - \frac{r^2}{x(x+z)} \right) \right\} \right]$$

(vii)

Surface Integrations for W_n^{-1} .

$$\text{x-face, } \int_S (u(r)\nabla_n u(r) + v(r)\nabla_n v(r))dS$$

| λ | A^2 | B^2 | AB | P^2 | Q^2 | PQ |
|-----------|---------|--------|--------|--------|-------|--------|
| 0.4 | 1.539 | .05402 | -.8973 | -.3627 | .1904 | .0330 |
| 0.6 | .00598 | .04163 | .5603 | -.3834 | .1302 | -.1249 |
| 0.8 | -0.8094 | .03172 | .3134 | -.3224 | .1001 | -.1863 |
| 1.0 | -1.0842 | .02405 | .1513 | -.2402 | .0610 | -.2176 |

$$\text{y-face, } \int_S v(r')\nabla_n u(r)dS$$

| λ | PA | PB | QA | QB |
|-----------|---------|-------|--------|-------|
| 0.4 | -2.052 | .5721 | .0296 | .1266 |
| 0.6 | -0.870 | .4215 | -.1544 | .0957 |
| 0.8 | -0.1590 | .3066 | -.2728 | .0727 |
| 1.0 | 0.2800 | .2075 | -.3084 | .0524 |

$$\text{y-face, } \int_S u(r')\nabla_n v(r)dS$$

| λ | PA | PB | QA | QB |
|-----------|--------|---------|--------|---------|
| 0.4 | -1.450 | -.02502 | -.5856 | -.08789 |
| 0.6 | -2.291 | -.01160 | -.2875 | -.05845 |
| 0.8 | -2.390 | .02383 | -.1372 | -.04460 |
| 1.0 | -2.181 | .04301 | -.0408 | -.02823 |

$$\text{y-face, } \int_S (u(r')\nabla_n v(r) - v(r')\nabla_n u(r))dS$$

| λ | PA | PB | QA | QB |
|-----------|--------|--------|--------|--------|
| 0.4 | 0.602 | -.5971 | -.6152 | -.2145 |
| 0.6 | -1.421 | -.4331 | -.1331 | -.1536 |
| 0.8 | -2.231 | -.2828 | .1336 | -.1173 |
| 1.0 | -2.461 | -.1645 | .2676 | -.0806 |

(viii)

$$J = \int_S \psi(r') \nabla_n \psi(r) \exp(i\mathbf{k} \cdot \frac{\mathbf{r}}{r}) dS \quad \text{for } W_p^2.$$

$$\psi(r) = u + iv$$

$$= \left\{ A \frac{P_x}{r} \frac{xy}{r^2} + B \frac{P_x}{r} \left(\frac{z^2 xy}{r^4} - \frac{1}{7} \frac{xy}{r^2} \right) + C \frac{P_x}{r} \left(\frac{x^2 - y^2}{r^4} xy \right) \right\} \\ + i \left\{ P_y \frac{y}{r} + Q \frac{y^3}{r^3} - \frac{3}{5} \frac{y}{r} + S \frac{P_x}{r} \left(\frac{z^2 - x^2}{r^3} y \right) \right\}$$

$\nabla_n u$ and $\nabla_n v$ for the x, y and z-faces were calculated in the same way as for W_p^1 and will not be written out explicitly in this case.

For the x-face

$$J = - \int_S u(r') \nabla_n u(r) dS + \int_S v(r') \nabla_n v(r) dS.$$

For the y-face

$$J = \int_S u(r') \nabla_n v(r) dS - \int_S v(r') \nabla_n u(r) dS$$

For the z-face

$$J = - \int_S u(r') \nabla_n v(r) dS - \int_S v(r') \nabla_n u(r) dS.$$

$$W_p^2, \underline{x\text{-face } u(r') \nabla_n u(r)}.$$

$$\text{Coefficient of } A^2 \quad \left[-\frac{P_2}{r} \frac{xz}{r^2} \right] \left[\frac{y+z}{r^2} \frac{x}{r} \left\{ \left(\frac{\partial P_2}{\partial r} - \frac{P_2}{r} \right) \frac{y}{r} + \frac{P_2}{r} \left(\frac{r}{y+z} - \frac{2y}{r} \right) \right\} \right]$$

$$\begin{aligned} \text{Coefficient of } B^2 \quad & \left[-\frac{P_2}{r} \left(\frac{zxy^2}{r^3} - \frac{1}{7} \frac{xz}{r^2} \right) \right] \left[\frac{y+z}{r} \frac{x}{r} \left\{ \left(\frac{\partial P_2}{\partial r} - \frac{P_2}{r} \right) \left(\frac{z^2 y}{r^2} - \frac{1}{7} \frac{y}{r} \right) \right. \right. \\ & \left. \left. + \frac{P_2}{r} \left(\frac{z}{r} \left(\frac{z+2y}{z+y} - \frac{4yz}{r^2} \right) - \frac{1}{7} \left(\frac{r}{y+z} - \frac{2y}{r} \right) \right) \right\} \right] \end{aligned}$$

$$\begin{aligned} \text{Coefficient of } C^2 \quad & \left[-\frac{P_2}{r} \left(\frac{x^2 z^2}{r^4} \right) \frac{xz}{r^2} \right] \left[\frac{y+z}{r^2} \frac{x}{r} \left\{ \left(\frac{\partial P_2}{\partial r} - \frac{P_2}{r} \right) \left(\frac{(x^2 - y^2)y}{r^2} \right) \right. \right. \\ & \left. \left. + \frac{P_2}{r} \left(\frac{r}{y+z} \left(\frac{x^2 - 3y^2}{r^2} - \frac{4y}{r} \left(\frac{x^2 - y^2}{r^2} \right) \right) \right) \right\} \right] \end{aligned}$$

$$\underline{x\text{-face } v(r') \nabla_n v(r)}$$

$$\text{Coefficient of } P^2 \quad \left[-\frac{P_2}{r} \frac{z}{r} \right] \left[\frac{y+z}{r^2} \left\{ \left(\frac{\partial P_2}{\partial r} - \frac{P_2}{r} \right) + \frac{P_2}{r} \left(\frac{r}{y+z} - \frac{y}{r} \right) \right\} \right]$$

$$\begin{aligned} \text{Coefficient of } Q^2 \quad & \left[-\frac{P_2}{r} \left(\frac{z^2}{r^2} - \frac{2}{5} \frac{z}{r} \right) \right] \left[\frac{y+z}{r^2} \left\{ \left(\frac{\partial P_2}{\partial r} - \frac{P_2}{r} \right) \left(\frac{y^2}{r^2} - \frac{2}{5} \frac{y}{r} \right) \right. \right. \\ & \left. \left. + 3 \frac{P_2}{r} \left(\frac{y^2}{r^2} - \frac{1}{5} \right) \left(\frac{r}{y+z} - \frac{y}{r} \right) \right\} \right] \end{aligned}$$

$$\begin{aligned} \text{Coefficient of } S^2 \quad & \left[-\frac{P_2}{r} \left(\frac{y^2 - x^2}{r^2} \right) \frac{z}{r} \right] \left[\frac{y+z}{r^2} \left\{ \left(\frac{\partial P_2}{\partial r} - \frac{P_2}{r} \right) \left(\frac{(z^2 - x^2)y}{r^2} \right) \right. \right. \\ & \left. \left. + \frac{P_2}{r} \left(\frac{z^2 - x^2 + 2zy}{r(y+z)} - 3y \left(\frac{z^2 - x^2}{r^2} \right) \right) \right\} \right] \end{aligned}$$

with cross-product terms $[AB]$ etc. formed as before

(x)

W_p^2 , y-face $v(r') \nabla_n u(r)$.

Coefficient of $[A_2]$ As for W_p^2 , $[A_2]$ with $\begin{pmatrix} x & y & z \\ y & x & z \end{pmatrix}$ on x-face.

" " $[B_2]$ " " " $[B_2]$ " " " "

" " $[C_2]$ " " " $[C_2]$ " " " " $x(-1)$.

" " $[P_1]$ " " W_p^1 $[P_1]$ " " " "

" " $[Q_1]$ " " " $[Q_1]$ " " " "

" " $[S_1] = \left[\frac{P_2}{r} y \left(\frac{x-z}{r^3} \right) \right]$

y-face $u(r') \nabla_n v(r)$

Coefficient of $[A_1]$ As for W_p^2 $[A_1]$ with $\begin{pmatrix} x & y & z \\ y & x & z \end{pmatrix}$ on x-face.

" " $[B_1]$ " " " $[B_1]$ " " " "

" " $[C_1]$ " " " $[C_1]$ " " " "

" " $[P_2]$ " " W_p^1 $[P_2]$ " " " "

" " $[Q_2]$ " " " $[Q_2]$ " " " "

" " $[S_2] = \left[\frac{x+z}{r^2} \frac{y}{r} \left(\frac{\partial P_2}{\partial r} - \frac{P_2}{r} \right) \frac{z^2-x^2}{r^2} + \frac{P_2}{r} \left(\frac{z^2-x^2}{r^2} + 2 \frac{x-z}{x+z} \right) \right]$

W_p^2 , z-face $v(r') \nabla_n u(r)$.

Coefficient of $[A_2]$ $\left[\frac{x+y}{r^2} \left\{ \left(\frac{\partial P_1}{\partial r} - \frac{P_1}{r} \right) \frac{xy}{r^2} + \frac{P_1}{r} \left(1 - \frac{2xy}{r^2} \right) \right\} \right]$

Coefficient of $[B_2]$ $\left[\frac{x+y}{r^2} \left\{ \left(\frac{\partial P_1}{\partial r} - \frac{P_1}{r} \right) \frac{xy}{r^2} \left(\frac{z^2}{r^2} - \frac{1}{7} \right) + \frac{P_1}{r} \left(\frac{z^2}{r^2} \left(1 - \frac{4xy}{r^2} \right) - \frac{1}{7} \left(1 - \frac{2xy}{r^2} \right) \right) \right\} \right]$

Coefficient of $[C_2]$ $\left[\frac{x+y}{r^2} \left\{ \left(\frac{\partial P_1}{\partial r} - \frac{P_1}{r} \right) \frac{xy}{r^2} \left(\frac{x^2-y^2}{r^2} \right) + \frac{P_1}{r} \left(\frac{2xy}{r^2} \left(\frac{x-y}{x+y} \right) + \frac{x^2-y^2}{r^2(x+y)} - \frac{4xy(x^2-y^2)}{r^4} \right) \right\} \right]$

Coefficient of $[P_1]$ As for W_p^1 , $[P_1]$ with $\begin{pmatrix} x & y & z \\ y & z & x \end{pmatrix}$ on y-face.

Coefficient of $[Q_1]$ As for W_p^1 , $[Q_1]$ with $\begin{pmatrix} x & y & z \\ y & z & x \end{pmatrix}$ on y-face.

Coefficient of $[S_1]$ As for W_p^2 , $[S_1]$ with $\begin{pmatrix} x & y & z \\ -z & y & x \end{pmatrix}$ on x-face.

z-face $u(r') \nabla_n v(r)$.

Coefficient of $[A_1]$ $\left[\frac{P_1}{r} \frac{xy}{r^2} \right]$

Coefficient of $[B_1]$ $\left[\frac{P_1}{r} \frac{xy}{r^2} \left(\frac{z^2}{r^2} - \frac{1}{7} \right) \right]$

Coefficient of $[C_1]$ $\left[\frac{P_1}{r} \frac{xy}{r^2} \left(\frac{y^2-x^2}{r^2} \right) \right]$

Coefficient of $[P_2]$ As for W_p^1 , $[P_2]$ with $\begin{pmatrix} x & y & z \\ y & z & x \end{pmatrix}$ on y-face.

Coefficient of $[Q_2]$ As for W_p^1 , $[Q_2]$ with $\begin{pmatrix} x & y & z \\ y & z & x \end{pmatrix}$ on y-face.

Coefficient of $[S_2]$ As for W_p^2 , $[S_2]$ with $\begin{pmatrix} x & y & z \\ -z & y & x \end{pmatrix}$ on x-face.

(xii)

Surface Integrations at W_D^2

$$\text{x-face} \quad - \int_S u(\mathbf{r}') \nabla_n u(\mathbf{r}) dS + \int_S v(\mathbf{r}') \nabla_n v(\mathbf{r}) dS$$

| λ | A^2 | B^2 | C^2 | AB | AC | BC |
|-----------|---------|----------|---------|---------|--------|--------|
| 0.4 | -.04907 | -.007706 | -.01310 | +.08930 | .14278 | .04076 |
| 0.6 | +.01904 | -.006269 | -.01066 | -.05476 | .09499 | .03216 |
| 0.8 | +.05519 | -.005479 | -.00871 | -.03205 | .05996 | .02433 |
| 1.0 | +.06487 | -.004372 | -.00691 | -.01342 | .03502 | .01246 |

| λ | P^2 | Q^2 | S^2 | PQ | PS | QS |
|-----------|--------|-------|--------|--------|--------|--------|
| 0.4 | .5229 | .5022 | -.7704 | -.4814 | 2.3594 | -.5540 |
| 0.6 | 1.0292 | .3316 | -.7264 | -.1839 | 1.0592 | -.2110 |
| 0.8 | 1.2271 | .2614 | -.6069 | .0516 | .2691 | -.1327 |
| 1.0 | 1.1138 | .1687 | -.3179 | .1926 | -.6634 | -.0458 |

$$\text{y-faces} \quad - \int_S v(\mathbf{r}') \nabla_n u(\mathbf{r}) dS$$

| λ | PA | PB | PC | QA | QB | QC | SA | SB | SC |
|-----------|---------|---------|--------|---------|---------|---------|---------|---------|---------|
| 0.4 | -.02852 | -.08623 | -.1560 | -.02095 | -.05684 | -.11340 | -.01552 | -.02284 | -.08616 |
| 0.6 | .03789 | -.06035 | -.1077 | .03281 | -.04373 | -.08660 | .01538 | -.01768 | -.06403 |
| 0.8 | .06615 | -.03950 | -.0557 | .06073 | -.03364 | -.06785 | .03496 | -.01417 | -.04893 |
| 1.0 | .06556 | -.02701 | -.0433 | .08191 | -.02936 | -.05683 | .04322 | -.00664 | -.03580 |

(iii)

$$y\text{-face } \int_S u(r') \nabla_n v(r) dS$$

| λ | PA | PB | PC | QA | QB | QC | SA | SB | SC |
|-----------|--------|---------|--------|-------|--------|---------|--------|--------|--------|
| 0.4 | -.4086 | -.04729 | .05559 | .2891 | .03380 | -.05020 | -.1780 | .04244 | .12038 |
| 0.6 | -.3856 | -.05051 | .07922 | .1735 | .02260 | -.03287 | -.1161 | .03128 | .08591 |
| 0.8 | -.3444 | -.04990 | .07943 | .1195 | .01565 | -.02472 | -.0799 | .02424 | .06667 |
| 1.0 | -.2840 | -.04723 | .07523 | .0380 | .01155 | -.01478 | -.0509 | .01785 | .04914 |

$$y\text{-face } \int_S u(r') \nabla_n v(r) dS - \int_S v(r') \nabla_n u(r) dS$$

| λ | PA | PB | PC | QA | QB | QC | SA | SB | SC |
|-----------|--------|---------|-------|--------|--------|--------|--------|--------|-------|
| 0.4 | -.3801 | .03894 | .2116 | .3101 | .09064 | .06320 | -.1625 | .06528 | .2065 |
| 0.6 | -.4235 | .00984 | .1869 | .1407 | .06633 | .05373 | -.1315 | .04896 | .1499 |
| 0.8 | -.4105 | -.01040 | .1352 | .0588 | .04929 | .04313 | -.1147 | .03841 | .1156 |
| 1.0 | -.3496 | -.02022 | .1185 | -.0431 | .04091 | .04205 | -.0942 | .02649 | .0849 |

$$z\text{-face } u(r') \nabla_n v(r) dS$$

| λ | PA | PB | PC | QA | QB | QC | SA | SB | SC |
|-----------|--------|---------|-------|--------|--------|-------|---------|--------|--------|
| 0.4 | .8115 | -.03227 | .2789 | -.3965 | .01077 | .2994 | -2.2407 | .08603 | .14602 |
| 0.6 | 1.3908 | -.05259 | .2903 | -.2741 | .01009 | .2008 | -1.4884 | .06485 | .09554 |
| 0.8 | 1.3825 | -.07033 | .3229 | -.2152 | .01012 | .1506 | -1.0956 | .05328 | .06916 |
| 1.0 | 1.3263 | -.07337 | .2721 | -.1460 | .00879 | .0654 | -.7136 | .03870 | .03428 |

(xiv)

$$x\text{-face } \int_S v(r') \nabla_n u(r) dS.$$

| λ | PA | PB | PC | QA | QB | QC | SA | SB | SC |
|-----------|--------|--------|-------|---------|--------|--------|-------|--------|--------|
| 0.4 | 2.2977 | -.3237 | .4468 | -.07584 | .01855 | -.4731 | .9253 | -.1384 | -.2163 |
| 0.6 | 1.2016 | -.2341 | .2996 | -.05563 | .01286 | -.3500 | .5316 | -.1094 | -.1606 |
| 0.8 | 0.4948 | -.1615 | .1873 | -.04515 | .01066 | -.2709 | .2642 | -.0890 | -.1245 |
| 1.0 | 0.1119 | -.1056 | .1078 | -.03646 | .00678 | -.1991 | .0824 | -.0700 | -.0918 |

$$z\text{-face } \int_S u(r') \nabla_n v(r) dS - \int_S v(r') \nabla_n u(r) dS$$

| λ | PA | PB | PC | QA | QB | QC | SA | SB | SC |
|-----------|---------|-------|--------|--------|---------|-------|---------|-------|-------|
| 0.4 | -1.4862 | .2913 | -.1679 | -.3207 | -.00778 | .7725 | -3.1661 | .2244 | .3623 |
| 0.6 | 0.1082 | .1915 | -.0094 | -.2185 | -.00277 | .5508 | -2.020 | .1743 | .2561 |
| 0.8 | 0.8877 | .0912 | .1356 | -.1700 | -.00054 | .4214 | -1.360 | .1423 | .1937 |
| 1.0 | 1.2145 | .0322 | .1643 | -.1096 | .00201 | .2645 | -0.796 | .1087 | .1261 |

y-faces and z-faces

| λ | PA | PB | PC | QA | QB | QC | SA | SB | SC |
|-----------|---------|--------|--------|-------|--------|--------|-------|--------|--------|
| 0.4 | 1.1061 | -.2524 | .3795 | .6307 | .09842 | -.7093 | 3.003 | -.1591 | -.1558 |
| 0.6 | 0.5317 | -.1817 | .1962 | .3592 | .06910 | -.4171 | 1.889 | -.1253 | -.1062 |
| 0.8 | -1.2982 | -.1016 | -.0004 | .2288 | .04983 | -.3783 | 1.245 | -.1039 | -.0781 |
| 1.0 | -1.5641 | -.0524 | -.0458 | .0665 | .03890 | -.2224 | 0.702 | -.0822 | -.0412 |

Potential for s-like wave functions.

| r | V | r | V | r | V |
|--------|---------|------|-------|-----|-----|
| (r.u.) | (Ry.) | | | | |
| .01 | 2526.47 | .42 | 23.96 | 1.9 | .77 |
| .02 | 1228.48 | .44 | 22.07 | 2.0 | .71 |
| .03 | 796.68 | .45 | 21.21 | 2.1 | .65 |
| .04 | 581.55 | .46 | 20.40 | 2.2 | .51 |
| .05 | 453.08 | .48 | 18.95 | 2.3 | .39 |
| .06 | 367.93 | .50 | 17.72 | 2.4 | .33 |
| .07 | 307.57 | .52 | 16.70 | 2.5 | .29 |
| .08 | 262.62 | .54 | 15.78 | 2.7 | .25 |
| .09 | 228.35 | .55 | 15.35 | 2.9 | .22 |
| .10 | 200.74 | .56 | 14.95 | 3.1 | .17 |
| .11 | 178.26 | .58 | 14.21 | 3.3 | .06 |
| .12 | 159.60 | .60 | 13.56 | 3.5 | .01 |
| .13 | 143.85 | .62 | 12.97 | 3.7 | .00 |
| .14 | 130.23 | .64 | 12.38 | | |
| .15 | 118.64 | .65 | 12.08 | | |
| .16 | 108.35 | .66 | 11.72 | | |
| .17 | 99.20 | .68 | 11.18 | | |
| .18 | 91.00 | .70 | 10.57 | | |
| .19 | 83.57 | .72 | 9.77 | | |
| .20 | 76.78 | .74 | 8.99 | | |
| .21 | 71.87 | .75 | 8.60 | | |
| .22 | 67.28 | .76 | 8.21 | | |
| .23 | 63.03 | .78 | 7.45 | | |
| .24 | 59.10 | .80 | 6.70 | | |
| .25 | 55.50 | .85 | 5.06 | | |
| .26 | 52.23 | .90 | 3.87 | | |
| .27 | 49.21 | .95 | 3.39 | | |
| .28 | 46.67 | 1.00 | 3.22 | | |
| .29 | 44.38 | 1.05 | 3.12 | | |
| .30 | 42.42 | 1.10 | 3.03 | | |
| .31 | 40.29 | 1.15 | 2.77 | | |
| .32 | 38.28 | 1.20 | 2.49 | | |
| .33 | 36.37 | 1.25 | 2.23 | | |
| .34 | 34.57 | 1.30 | 2.01 | | |
| .35 | 32.88 | 1.35 | 1.86 | | |
| .36 | 31.30 | 1.40 | 1.74 | | |
| .37 | 29.83 | 1.50 | 1.53 | | |
| .38 | 28.46 | 1.60 | 1.30 | | |
| .39 | 27.21 | 1.70 | 1.09 | | |
| .40 | 26.06 | 1.80 | .91 | | |

Potential for p-like wave functions.

| r | V | r | V | r | V |
|--------|--------|------|-------|------|------|
| (a.u.) | (Ry.) | | | | |
| .002 | 12924 | .33 | 36.22 | 1.05 | 3.01 |
| .004 | 6424 | .34 | 34.45 | 1.1 | 2.94 |
| .006 | 4258 | .35 | 32.81 | 1.15 | 2.69 |
| .008 | 3165 | .36 | 31.29 | 1.2 | 2.41 |
| .010 | 2525.5 | .37 | 29.85 | 1.25 | 2.17 |
| .012 | 2092.1 | .38 | 28.52 | 1.3 | 1.95 |
| .014 | 1782.6 | .39 | 27.27 | 1.35 | 1.81 |
| .016 | 1550.7 | .40 | 26.10 | 1.4 | 1.71 |
| .018 | 1370.4 | .41 | 25.00 | 1.45 | 1.61 |
| .02 | 1226.2 | .42 | 23.97 | 1.5 | 1.51 |
| .03 | 794.2 | .43 | 23.01 | 1.6 | 1.29 |
| .04 | 578.8 | .44 | 22.10 | 1.7 | 1.08 |
| .05 | 450.2 | .45 | 21.25 | 1.8 | .91 |
| .06 | 364.8 | .46 | 20.46 | 1.9 | .76 |
| .07 | 304.2 | .47 | 19.71 | 2.0 | .64 |
| .08 | 259.1 | .48 | 19.02 | 2.1 | .54 |
| .09 | 224.3 | .49 | 18.37 | 2.2 | .45 |
| .10 | 196.7 | .50 | 17.76 | 2.3 | .39 |
| .11 | 174.3 | .52 | 16.70 | 2.4 | .33 |
| .12 | 155.8 | .54 | 15.80 | 2.5 | .29 |
| .13 | 140.4 | .55 | 15.41 | 2.6 | .25 |
| .14 | 127.2 | .56 | 15.01 | 2.7 | .22 |
| .15 | 116.0 | .58 | 14.27 | 2.8 | .19 |
| .16 | 106.3 | .60 | 13.62 | 2.9 | .17 |
| .17 | 97.83 | .62 | 12.99 | 3.1 | .12 |
| .18 | 90.41 | .64 | 12.41 | 3.3 | .06 |
| .19 | 83.86 | .65 | 12.14 | 3.5 | .01 |
| .20 | 78.05 | .66 | 11.84 | 3.7 | .00 |
| .21 | 72.75 | .68 | 11.23 | | |
| .22 | 67.98 | .70 | 10.63 | | |
| .23 | 63.66 | .72 | 9.86 | | |
| .24 | 59.73 | .74 | 9.03 | | |
| .25 | 56.16 | .75 | 8.59 | | |
| .26 | 52.89 | .76 | 8.20 | | |
| .27 | 49.90 | .78 | 7.41 | | |
| .28 | 47.16 | .80 | 6.64 | | |
| .29 | 44.64 | .85 | 4.96 | | |
| .30 | 42.31 | .90 | 3.73 | | |
| .31 | 40.13 | .95 | 3.25 | | |
| .32 | 38.10 | 1.00 | 3.08 | | |

References.

- Bouckaert, Smoluchowski & Wigner 1936 Phys. Rev. 50, 58.
- Buckingham 1957 Numerical Methods, Pitman.
- Eyring, Walter & Kimball 1944 ^{Quantum} ~~Theoretical~~ Chemistry, Wiley.
- Gunnerson 1957 Phil. Trans. A, 249, 299.
- Heine 1957 Proc. Roy. Soc. A, 240, 340.
- Herman 1958 Rev. Mod. Phys. 30, ~~102~~
- Howarth & Jones 1952 Proc. Phys. Soc. A, 65, 355.
- Jenkins & Pincherle 1954 Phil. Mag. 45, 93.
- Jenkins 1954 Physica 20, no.11.
- Kittel 1953 Solid State Physics, Wiley.
- Kohn 1952 Phys. Rev., 82, 472.
- Margenau & Murphy 1943 Mathematics of Physics & Chemistry, D. van Nostrand.
- Mott & Jones 1936 Properties of Metals & Alloys, Clarendon Press.
- Pines 1955 Solid State Physics, Academic Press.
- Slater 1951 Phys. Rev. 81, 385.